arXiv:astro-ph/0512510v1 20 Dec 2005

Chemical Composition of the Planet-Harboring Star TrES-1

Alessandro Sozzetti[1,2], David Yong[3], Bruce W. Carney[3], John B. Laird[4], David W. Latham[1], and Guillermo Torres[1]

asozzett@cfa.harvard.edu

yong@physics.unc.edu

bruce@physics.unc.edu

laird@tycho.bgsu.edu

dlatham@cfa.harvard.edu

gtorres@cfa.harvard.edu

ABSTRACT

We present a detailed chemical abundance analysis of the parent star of the transiting extrasolar planet TrES-1. Based on high-resolution Keck/HIRES and HET/HRS spectra, we have determined abundances relative to the Sun for 16 elements (Na, Mg, Al, Si, Ca, Sc, Ti, V, Cr, Mn, Co, Ni, Cu, Zn, Y, and Ba). The resulting average abundance of $< [X/\mathrm{H}] > = -0.02 \pm 0.06$ is in good agreement with initial estimates of solar metallicity based on iron. We compare the elemental abundances of TrES-1 with those of the sample of stars with planets, searching for possible chemical abundance anomalies. TrES-1 appears not to be chemically peculiar in any measurable way. We investigate possible signs of selective accretion of refractory elements in TrES-1 and other stars with planets, and find no statistically significant trends of metallicity $[X/\mathrm{H}]$ with condensation temperature T_c. We use published abundances and kinematic information for the sample of planet-hosting stars (including TrES-1) and several statistical

[1]Harvard-Smithsonian Center for Astrophysics, 60 Garden Street, Cambridge, MA 02138 USA

[2]INAF - Osservatorio Astronomico di Torino, 10025 Pino Torinese, Italy

[3]Department of Physics & Astronomy, University of North Carolina at Chapel Hill, Chapel Hill, NC 27599 USA

[4]Department of Physics & Astronomy, Bowling Green State University, Bowling Green, OH 43403 USA

indicators to provide an updated classification in terms of their likelihood to belong to either the thin disk or the thick disk of the Milky Way Galaxy. TrES-1 is found to be a very likely member of the thin disk population. By comparing α-element abundances of planet hosts and a large control sample of field stars, we also find that metal-rich ([Fe/H]$\gtrsim 0.0$) stars with planets appear to be systematically underabundant in [α/Fe] by ≈ 0.1 dex with respect to comparison field stars. The reason for this signature is unclear, but systematic differences in the analysis procedures adopted by different groups cannot be ruled out.

Subject headings: Galaxy: solar neighborhood — stars: abundances — stars: kinematics — stars: individual (GSC 02652-01324) — planetary systems

1. Introduction

The possibility that super-solar metallicity could imply a higher likelihood of a given star to harbor a planet was investigated since the first detections by precision radial-velocity surveys (Gonzalez 1997, 1998a, 1998b; Fuhrmann et al. 1997, 1998; Laughlin & Adams 1997). A number of studies have been performed throughout these years, with increasingly larger sample sizes, employing both spectroscopic and photometric techniques for metallicity determination (using iron as the primary reference element), and adopting control samples of field stars without detected planets (Santos et al. 2000, 2001, 2003, 2004a, 2005; Reid 2002; Laughlin 2000; Gonzalez & Laws 2000; Gonzalez et al. 2001; Israelian et al. 2001; Queloz et al. 2000a; Smith et al. 2001; Giménez 2000; Martell & Laughlin 2002; Heiter & Luck 2003; Sadakane et al. 2002; Pinsonneault et al. 2001; Murray & Chaboyer 2002; Laws et al. 2003; Fischer & Valenti 2005).

The global trend is that planet-harboring stars are indeed more metal rich than stars without known planets. Based on observationally unbiased stellar samples, the strong dependence of planetary frequency on the host star metallicity has been clearly demonstrated by e.g., Santos et al. (2001, 2004a), and Fischer & Valenti (2005). Furthermore, the metallicity enhancement is likely to be "primordial" in nature, i.e. due to the intrinsically high metal content of the protoplanetary cloud from which the planetary systems formed, as opposed to the possibility of "self-enrichment", caused by accretion of rocky planetesimal material onto the parent star (see Gonzalez 2003 for a review of the subject). This conclusion is primarily based upon the evidence of no dependence of the iron-abundance enhancement on the stellar effective temperature, as theoretical calculations would predict (e.g., Dotter & Chaboyer 2003; Cody & Sasselov 2005, and references therein, but see also Vauclair 2004 for somewhat different arguments), and it bears important consequences

for the proposed models of giant planet formation by core accretion (e.g., Ida & Lin 2005; Kornet et al. 2005) and disk instability (Boss 2002).

Based on detailed chemical abundance analyses of metals other than iron, several attempts have been made in the recent past to confirm the observed trend and to put on firmer grounds (or refute) the idea that stars with planets are primordially metal-rich, and have not been polluted. Many authors have determined the abundances of over a dozen other elements for planet hosts, including light elements such as Li and the isotopic ratio ^{6}Li/^{7}Li (Gonzalez & Laws 2000; Ryan 2000; Israelian et al. 2001, 2003, 2004; Reddy et al. 2002; Mandell et al. 2004) and Be (García López & Pérez de Taoro 1998; Deliyannis et al. 2000; Santos et al. 2002, 2004b), refractories such as the α-elements Si, Mg, Ca, Ti, and the iron-group elements Cr, Ni, and Co, and volatiles such as C, N, O, S, and Zn (Santos et al. 2000; Gonzalez et al. 2001; Smith et al. 2001; Takeda et al. 2001; Sadakane et al. 2002; Zhao et al. 2002; Bodaghee et al. 2003; Ecuvillon et al. 2004a, 2004b, 2005a; Beirão et al. 2005; Gilli et al. 2005).

For instance, detection of anomalous light-element abundances in the atmosphere of a star could be indicative of recent planetary accretion events. While evidence for Li excesses in some planet-harboring stars has been reported in the literature (Israelian et al. 2001, 2003; Laws & Gonzalez 2001), clearly suggesting that accretion of planetary material can actually take place in some stars, as implied by theoretical arguments (Montalbán & Rebolo 2002; Boesgaard & King 2002; Sandquist et al. 2002), in general stars with planets have normal light-element abundances, typical of field stars (e.g., Ryan 2000; Israelian et al. 2004).

Arguments in favor of the "self-enrichment" hypothesis could also be substantiated if volatile elements were to exhibit different abundance trends with respect to refractory elements. One way to approach the problem is to make use of the condensation temperatures T_c of the elements, a typical diagnostic employed for investigating chemical fractionation patterns in many areas of planetary science and astronomy (e.g., Lodders 2003, and references therein). In this particular case, volatiles, having low T_c-values, are expected to show a deficiency in accreted material with respect to refractories. However, the most recent evidence (e.g., Bodaghee et al. 2003; Ecuvillon et al. 2004a, 2004b, 2005a; Gilli et al. 2005) is that the abundance distributions of other elements in stars with planets are simply the extension of the observed behavior for [Fe/H], a result quantified by trends of decreasing [X/Fe] with increasing [Fe/H], for both refractories and volatiles. It thus seems unlikely that pollution effects can be responsible for the overall metallicity enhancement of the planet host stellar sample.

The primary goal of this work is to present a detailed study of the chemical composition of the parent star of the recently discovered transiting extrasolar planet TrES-1 (GSC 02652-

01324; Alonso et al. 2004). We have done so by undertaking a detailed chemical abundance analysis using our Keck and Hobby Eberly Telescope (HET) spectra of TrES-1. Secondly, we have compared the elemental abundances of TrES-1 with those of the sample of stars with planets, in order to search for possible chemical abundance anomalies in the former. To this end, we have utilized results from uniform studies of elemental abundances of large sets of planet hosts available in the literature. Third, in an attempt to find circumstantial evidence of possible selective accretion of planetary material, we have further investigated the sample of planet hosts and TrES-1, searching for statistically significant trends of $[X/\mathrm{H}]$ with condensation temperature. Finally, we have utilized the chemical composition information for TrES-1 and a large sample of planet-hosting stars along with their kinematic properties in order to classify them, based on a number of diagnostic indicators, in terms of their likelihood of being members of the thin or thick disk populations of the Milky Way Galaxy (e.g., Gilmore & Reid 1983; Carney et al. 1989. See Majewski 1993, and references therein, for a comprehensive review and discussion of formation scenarios). This analysis has the purpose of revisiting and updating the results of a few past studies (Gonzalez 1999; Reid 2002; Barbieri & Gratton 2002; Santos et al. 2003) which, using limited sample sizes, confirmed the strong similarity between the kinematic properties of stars with planets and that of control samples of stars without known planets.

This paper is organized as follows. In Section 2 we present our chemical abundance analysis for the planet-hosting star TrES-1. All elemental abundances are compared in Section 3 with those of selected, uniformly studied samples of planet hosts. Section 4 is dedicated to an updated classification of planet-harboring stars in terms of different stellar populations in our Galaxy. Finally, Section 5 contains a summary of the main results and concluding remarks.

2. Observations and Abundance Analysis

The Keck/HIRES and HET/HRS spectra analyzed in this paper have been studied by Sozzetti et al. (2004) for an improved determination of the stellar and planetary parameters of the system. We refer the reader to that paper for a description of the data.

2.1. Abundances

The abundance analysis of TrES-1 in the spectral region 3820-7840 Å covered by our data was carried out using a modified version of the local thermodynamic equilibrium (LTE)

spectral synthesis code MOOG (Sneden 1973) and a grid of Kurucz (1993) LTE model stellar atmospheres. Overall, we present here results for 16 additional elements (Na, Mg, Al, Si, Ca, Sc, Ti, V, Cr, Mn, Co, Ni, Cu, Zn, Y, and Ba), plus Fe and Li which had already been the subject of study in the Sozzetti et al. (2004) paper. Our set of elements spans a range of condensation temperatures of about 1000 K, the element with the lowest T_c being Zn. Zinc is notably interesting for at least two reasons. For instance, this element is commonly used to investigate abundance patterns between different stellar populations resulting from chemical evolution processes in our Milky Way Galaxy (Sneden et al. 1991; Prochaska et al. 2000; Bensby et al. 2003). The accurate determination of the abundance ratio [Zn/Fe] is also of great importance in studies addressing questions on the chemical evolution of the early universe, which employ quasar absorption line abundance analyses, in particular damped Lyα systems, believed to be the progenitors of modern galaxies (e.g., Prochaska & Wolfe 2000, and references therein). Recent studies (e.g., Mishenina et al. 2002; Bensby et al. 2003; Ecuvillon et al. 2004b; Nissen et al. 2004. See Chen et al. (2004) for a review of the subject of Zn abundances determination) have provided indications that Zn might not be an exact tracer of Fe, as it is often assumed. Unfortunately, attempts to measure abundances for other important volatiles, such as C, N, O, and S, with even lower T_c-values, were not successful, the limiting factors being the fact that TrES-1 is cool and not metal-poor, thus lines of these elements are too strong and lie in regions too crowded to be analyzed, or they are outside our wavelength coverage.

For each element in the spectrum for which at least one relatively weak, unblended line could be found, we determined equivalent widths (EW) using the SPLOT task in IRAF[1]. Abundances were computed using the ABFIND driver in MOOG, and by imposing excitation and ionization equilibrium (e.g., Sozzetti et al. 2004; Santos et al. 2004a, and references therein). The solar abundances of reference were taken from Grevesse & Sauval (1998). Hyperfine and isotopic splitting was taken into account for Sc, V, Mn, Co, Cu, and Ba. In our analyses, with the exception of Cu, for which a line list from Simmerer et al. (2003) was utilized, we adopted the hyperfine line lists from Prochaska et al. (2000), and solar isotopic ratios (Anders & Grevesse 1989) . In four cases (Mg, Al, Cu, and Zn), all the lines in the spectral domain of our data were slightly blended and/or in regions where the continuum was difficult to determine such that an EW analysis would not give reliable results. For these four elements, abundances were obtained by fitting synthetic spectra to the data. In the panels of Figure 1 we show two examples of spectral synthesis for Al I and Zn I lines, respectively.

[1]IRAF is distributed by the National Optical Astronomy Observatories, operated by the Association of Universities for Research in Astronomy, Inc., under contract with the National Science Foundation, USA.

For each element analyzed, we summarize in Table 1 the final list of lines adopted, the lower excitation potentials, the oscillator strength values and the literature sources from which they were taken, and the relative EWs (where applicable). The abundance ratios $[X/\mathrm{Fe}]$ (and [Fe/H]) for each element, averaged over all useful lines, are presented in Table 2, along with the actual number of lines used in each case. The quoted errors correspond to the dispersion around the mean. Finally, in Figure 2 we plot the elemental abundances of TrES-1, expressed as $[X/\mathrm{H}]$, as a function of element number. Iron is included, but not lithium, for which only an upper limit had been obtained by Sozzetti et al. (2004). As one can see, the mean abundance ratio for this star ($<[X/\mathrm{H}]>= -0.02$, indicated by the horizontal solid line, with a dispersion of ± 0.06 dex) is very similar to solar, confirming the first estimates by Sozzetti et al. (2004), who used iron as a proxy.

2.2. Sources of Uncertainty

Abundance determinations can be subject to a significant number of uncertainties, which can be random or systematic in nature. For example, EWs can be measured incorrectly due to unrecognized blends or poor location of the continuum, a problem that can become severe when only a few lines are available for a given element. When a large set of lines can be found, then uncertainties in the determination of stellar atmospheric parameters (effective temperature $T_{\rm eff}$, surface gravity $\log g$, and microturbulent velocity ξ_t) are more likely to constitute the more significant sources of error in the abundance determination for a given species. Sozzetti et al. (2004) have derived (following the prescriptions of Neuforge & Magain (1997) and Gonzalez & Vanture (1998)) errors in $T_{\rm eff}$, $\log g$, and ξ_t of ± 75 K, ± 0.2 dex, and ± 0.10 km s^{-1}, respectively. In Table 3 we show the sensitivity of the abundances for all elements measured in TrES-1 to changes of the above amounts in the atmospheric parameters, with respect to the nominal values of $T_{\rm eff} = 5250$ K, $\log g = 4.6$, and $\xi_t = 0.95$ km s^{-1} (Sozzetti et al. 2004). In most cases, variations are comparable to, or smaller than, the quoted uncertainties in Table 2.

Finally, non-LTE effects have not been taken into account in our analysis. In principle, systematic uncertainties can arise due to the use of plane-parallel, LTE model atmospheres. This issue has been a matter of debate for quite some time. Recent studies argue that non-LTE effects are particularly strong in very cool and metal-poor stars (e.g, Edvardsson et al. 1993; Feltzing & Gustafsson 1998; Thévenin & Idiart 1999; Chen et al. 2000; Yong et al. 2004). For stars with the temperature (or higher) and metallicity (or higher) of TrES-1, such corrections are typically of the same order (or smaller) than the quoted uncertainties from our abundance analyses. We thus believe that ignoring non-LTE effects

in the analysis has not introduced any major source of error.

3. TrES-1 vs. Other Planet Hosts

We attempt here to put TrES-1 in context with the other planet-bearing stars known today. In particular, we have searched for 1) possible chemical abundance anomalies, by comparing the abundances in TrES-1 with those determined for other stars with planets, and 2) possible signs of selective accretion of refractory elements and chemical evolutionary effects, by analyzing the dependence of abundances on condensation temperature T_c for both TrES-1 and the sample of planet hosts.

3.1. Comparison Between Abundance Ratios

The Jupiter-sized transiting planet found orbiting TrES-1 (Alonso et al. 2004) is the first success of wide-field, ground-based photometric surveys which target relatively bright ($9 \lesssim V \lesssim 13$) stars, typically lying at a few hundred pc from the Sun (for a review see for example Horne 2004 and Charbonneau 2004). These samples have little or no distance overlap with that of solar-neighborhood stars ($D < 50-100$ pc) targeted by Doppler surveys. On the one hand, the evidence for a mild radial metallicity gradient of ~ -0.09 dex/kpc in the disk of the Milky Way presented by Nordström et al. (2004) suggests that, when attempting to undertake statistical studies of possible correlations between planet properties and the chemical abundances of the host stars (e.g., Sozzetti 2004, and references therein) using stellar samples covering a distance range of hundreds of pc, large-scale metallicity trends should also be taken into account, in order to cope with this potential bias. On the other hand, based on the photometric distance estimate of ~ 150 pc for TrES-1 inferred by Sozzetti et al. (2004) and Laughlin et al. (2005), one could *a priori* expect that no significant anomalies should be found for this object in particular. One way or the other, it is thus beneficial to carry out the experiment to compare the chemical composition of planet-hosts discovered by radial-velocity surveys and that of TrES-1 presented in this work. Our study is illustrative of those that will be undertaken to better characterize the parent stars of all transiting planets that will likely be found in the coming years by the large number of ongoing and planned wide-field, ground-based photometric surveys.

We have collected chemical composition information for stars with planets from a variety of literature sources. The results we have utilized in our comparison have all been obtained in the context of systematic, uniform, and detailed spectroscopic studies of large sets of planet-

harboring stars. We present in Figures 3 and 4, in the plane $[X/H]$-[Fe/H], the comparison between the abundances for 16 elements measured in TrES-1 and those obtained for other planet hosts. Except for one case, every element measured in TrES-1 has been compared with the same element measured in a large subset of planet hosts in the context of a single study (see captions of Figures 3 and 4). In this way, we have attempted to minimize the possibility that unknown systematics may have been introduced by considering for each element a set of results from a variety of studies which used different spectral line lists and model atmospheres to derive stellar parameters and abundances.

As a general remark, TrES-1 does not appear to be anomalous in any conspicuous way. All abundance estimates for the elements appear to be rather 'normal'. The only possible exception is Chromium, which appears to be slightly overabundant. However, in the TrES-1 spectra we could locate only one measurable line for Cr I, and none for Cr II. The possibility of an unrecognized blend in the measurement of the EW for the 5238.96 Å Chromium line cannot be ruled out. Alternatively, although the general features of the spectroscopic abundance determination are similar, systematic differences in the details of the analysis carried out in this work and that of Bodaghee et al. (2003) could also contribute to explain the observed discrepancy. The first possible systematic difference to look for between the Bodaghee et al. (2003) and our analyses is the $\log gf$ value. Our Cr I line was not used by Bodaghee et al. (2003), nor were any of Bodaghee's Cr I lines in the Thorén & Feltzing (2000) paper from which we took our $\log gf$ value. Therefore, we suspect an offset in $\log gf$ values but cannot track it down since there are no lines in common between the studies. We note, however, that for all other elemental abundances in TrES-1 for which we have used the Bodaghee et al. (2003) sample for comparison no anomaly is apparent.

3.2. Signatures of Accretion

In order to find possible circumstantial evidence of accretion of metal-enriched material onto the parent star, Sozzetti et al. (2004) attempted to measure the Li abundance in TrES-1, but could place only a low upper limit of $\log \epsilon(\mathrm{Li}) < 0.1$. A comparison of the result for TrES-1 with other Li abundance estimates for planet hosts obtained by Israelian et al. (2004) is presented in Figure 5. As one can see, TrES-1 appears not to be peculiar in any measurable way, further corroborating the conclusion that no recent accretion events have occurred in this star.

Another test that has been proposed to investigate further (in a statistical sense) the idea of planetesimal accretion is to search for evidence of a dependence between elemental abundances $[X/H]$ and condensation temperature T_c. As any accretion events would occur in

a high temperature environment (very close to the star), refractories which condense at high T_c (e.g., α-group and iron-peak elements) might be added in larger quantities with respect to volatiles with much lower T_c (e.g., C, N, O, and Zn). A further constraint in this case is for enrichment not to occur rapidly, so as to give sufficient time to volatile elements to evaporate, otherwise any possible chemical differentiation might not be detectable. We show in Figure 6 abundances $[X/\mathrm{H}]$ as a function of T_c for TrES-1. Any trend of $[X/\mathrm{H}]$ with T_c can be quantified in terms of a significant positive slope in a linear least-squares fit. In our case (solid line in Figure 6) the derived slope of $2.74(\pm6.80) \times 10^{-5}$ dex K^{-1} is statistically insignificant, thus no measurable correlation between chemical abundances and T_c is found. We note, however, that the element with the lowest abundance (Zn) is also the one with the lowest T_c. We are fully aware of the importance of extending the range of condensation temperatures to put our results on more solid grounds. Unfortunately, as discussed before, we have not been able to measure reliable abundances for C, N, O, and S within the Keck and HET spectra. Additional very high resolution, very high S/N spectroscopic observations of TrES-1 (possibly extending to the infrared to study molecular line features of CO, CN, and OH), aimed at studying volatiles and refractories with a very wide range of condensation temperatures, are clearly encouraged.

Based on relatively small sample sizes of stars with planets, the possibility of a trend of $[X/\mathrm{H}]$ with T_c has been investigated in the past by several authors (Gonzalez 1997; Smith et al. 2001; Takeda et al. 2001; Sadakane et al. 2002). In particular, Smith et al. (2001), by comparing a set of planet hosts studied by Gonzalez et al. (2001) and of field dwarfs without known planets from the Edvardsson et al. (1993) and Feltzing & Gustafsson (1998) surveys, showed a trend of decreasing T_c-slope with [Fe/H], explained in terms of Galactic chemical evolution. They then highlighted a small number of high-metallicity stars with planets exhibiting positive T_c-slopes above the established trend, and suggested these might be good candidates to have undergone selective accretion of planetary material. However, Smith et al. (2001) pointed out that the heterogeneity of the data utilized for the analysis prevented them from drawing more than tentative conclusions. Takeda et al. (2001) and Sadakane et al. (2002), on the other hand, conducted independent abundance analyses of a couple dozen planet hosts and a handful of planetless field stars, including some from the Gonzalez et al. (2001) sample which, according to Smith et al. (2001), showed signs of a correlation between chemical abundances and T_c, and concluded that no statistically convincing trend could be found. Due to the very small number of comparison field stars observed, the conclusions they draw can only be considered suggestive.

In an attempt to improve on the above results, we have revisited this issue by determining the T_c-slopes for a set of ~ 100 planet-harboring stars and ~ 40 stars not known to have planets, utilizing the abundances presented in the large, uniform studies of Bodaghee et al.

(2003), Ecuvillon et al. (2004a, 2004b, 2005a), and Beirão et al. (2005). While the sample of comparison field stars is smaller by a factor ~ 2 with respect to those utilized by Smith et al. (2001), and it does not extend to quite as low metallicities, it has the crucial advantage of having been analyzed by the same group, thus possible systematics arising from the comparison between different analysis methods should be avoided. However, in their study Bodaghee et al. (2003) utilized the atmospheric parameters and iron abundances from Santos et al. (2000, 2001, 2003), while the works of Ecuvillon et al. (2004a, 2004b, 2005a), and Beirão et al. (2005) used updated values from Santos et al. (2004a) and Pepe et al. (2004). In order to assess the impact of possible residual systematic differences, we compared the $T_{\rm eff}$ and [Fe/H] values for stars with planets in common between the two studies. The effective temperature is the most critical parameter, and in this case the different values adopted by Bodaghee et al. and Ecuvillon et al. and Beirao et al., respectively, are in excellent agreement with each other, with a mean difference $\Delta T_{\rm eff} = -3$ K and a standard deviation of 34 K. Such a difference is not expected to affect abundances. Indeed, the average difference Δ[Fe/H] in the two studies is null, with a dispersion of 0.03 dex. No trends of Δ[Fe/H] vs. [Fe/H] are found, as shown in Figure 7. Thus, the datasets from Bodaghee et al. and Ecuvillon et al. and Beirao et al. may be safely combined.

In the abovementioned works, abundances were determined for elements covering a large range of condensation temperatures (low values of T_c as for C, N, and O, intermediate values as for S, Cu, Zn, and Na, and high values as for Fe, Mg, Ti, and Ca). We show the derived values of the T_c-slopes (including the one for TrES-1 obtained in this work) in Figure 8, as a function of [Fe/H]. First, as shown by the the straight line through the points, only a weak trend of decreasing T_c-slope with decreasing [Fe/H] can be detected (the linear least-squares fit has a slope of $4.65(\pm3.01) \times 10^{-5}$ K^{-1}). The lack of a measurable T_c-[Fe/H] trend, to be interpreted as a signature of Galactic disk chemical evolution, is likely due to the metallicity range encompassed by the data utilized in the analysis. In fact, the vast majority of the field stars from the Edvardsson et al. (1993) survey with [Fe/H]$\lesssim -0.6$ have negative T_c-slopes in Figure 10 of Smith et al. (2001), while the planet hosts and control samples used here do not extend below [Fe/H]$\simeq -0.5$.

Second, the average and dispersion of the T_c-slopes of the combined sample shown in Figure 8 are $4.79(\pm8.23) \times 10^{-5}$ dex K^{-1}. Taking into account uncertainties on the T_c-slopes, three planet hosts (HD 40979, HD 162020 and HD 222404) and three comparison field stars (HD 23356, HD 50281, and HD 191408) deviate by $2-3\sigma$ from the average. This is, however, far from being a statistically firm result, and these objects do not appear to cluster at large [Fe/H], but rather span a range of metallicities $-0.5 \lesssim$[Fe/H]$\lesssim 0.2$. In addition, none of the stars suggested by Smith et al. (2001) to be candidates to have undergone selective accretion of refractory elements shows significant positive slopes. The

magnitude of the effect shown by Smith et al. (2001) is relatively small, and the presence of systematics between the methods for abundance determinations adopted by different authors in the Smith et al. (2001) sample and the one utilized in this work could easily be invoked to explain this difference. Furthermore, as suggested by Gonzalez (2003), evidence for self-enrichment resulting from large T_c-slopes should also translate into trends with $T_{\rm eff}$, the hottest stars displaying the largest slope values. We show in Figure 9 the T_c-slopes as a function of $T_{\rm eff}$ for the combined sample utilized in the analysis. Indeed, a weak trend with a *negative* slope of $-0.005(\pm0.002) \times 10^{-5}$ dex K^{-2} (of statistically low significance) appears to be present in the opposite direction (the objects with largest slopes being the coolest). However, we interpret this feature as mostly due to the intrinsic difficulty to very accurately determine abundances for a large set of elements in cool stars ($T_{\rm eff} \lesssim 5000$ K) without the danger of introducing greater uncertainties in the abundance results and systematic errors primarily caused by departure from LTE, granulation convective motions, and crowdedness of the spectra.

In conclusion, the absence of any statistically convincing evidence for differences in the relative abundances of volatiles compared to refractories is one more piece of circumstantial evidence which indicates that pollution by accreted planetary material is not likely to play a significant role in the observed metallicity enhancement of stars with detected planets. Our findings are generally in agreement with the results presented in similar studies recently undertaken by Ecuvillon et al. (2005b, 2005c), in which a larger comparison sample is being used, with revised abundances (Gilli et al. 2005) for a significant number of elements for both stars with and without known planets. Condensation temperature trends among stars with planets have also been recently investigated by Gonzalez (2005) who, similarly to this work, also used a homogeneous set of published abundance data. In that paper, Gonzalez (2005) comes essentially to our same conclusions. In their series of papers on elemental abundance determinations for a large subset of planet-harboring stars and a control sample of stars without planets, Bodaghee et al. (2003), Santos et al. (2004a, 2004b, 2005), Ecuvillon et al. (2004a, 2004b, 2005a), Beirão et al. (2005, and Gilli et al. (2005)) drew similar conclusions, studying separately abundance trends for various elements and concluding that each abundance distribution for planet hosts is indistinguishable from that of the comparison sample, the former simply being the extension of the latter at high metallicities. Our result is also in line with the recent findings by Fischer & Valenti (2005) and Valenti & Fischer (2005), who could not detect any abundance variations for Na, Si, Ti, and Ni as a function of condensation temperature in a sample of 1040 FGK-type stars with and without planets from the Keck, Lick, and Anglo-Australian Telescope planet search programs. This conclusion is further corroborated by the observed trend from studies of the Li and Be abundances in planet hosts (as discussed in the introduction and at the beginning of this Section), and by

the evidence for no dependence of metallicity on the stellar convective envelope mass, as extensively discussed by e.g. Pinsonneault et al. (2001) and Fischer & Valenti (2005).

4. TrES-1, Other Planet Hosts, and Stellar Populations

Elemental abundances and galactic kinematics are often used to assign, on an observational basis, individual objects to different stellar populations in the Milky Way Galaxy. A few studies have concentrated on comparing the kinematics of planet hosts with that of comparison samples of field stars (Gonzalez 1999; Barbieri & Gratton 2002; Santos et al. 2003). No statistically significant kinematic peculiarity was uncovered between stars with and without known planets, the former simply being more metal-rich on average than the latter at any given distance from the galactic center. We focus here instead on assigning, in a statistical sense, TrES-1 to be either a thin- or thick-disk object, by comparison with other planet-bearing stars and a large sample of field stars. Whether a star belongs to one or the other galactic disk population has been determined on the basis of the agreement between a few indicators, which are purely kinematic in nature, a combination of kinematics and chemistry, or are solely chemistry-based.

4.1. Kinematic Indicators

While TrES-1 lacks a parallax estimate, photometric distances have been derived by Sozzetti et al. (2004) and Laughlin et al. (2005), which place the star+planet system at $d \approx 150$ pc. The combination of distance, proper motion, and radial-velocity allows one to calculate the galactic velocity vector (U, V, W, with U positive toward the galactic anti-center) with respect to the Local Standard of Rest (LSR), adjusting for the standard solar motion ($U_\odot$, $V_\odot$, $W_\odot$) = (-9.0,+12.0,+7.0) km s^{-1} (following Mihalas & Binney (1981)). The basic data are summarized in Table 4 (columns 1 through 10), together with the same information for a sample of 120 stars with planets.

One way to classify TrES-1 as either a thin or thick disk object is to use statistical indicators purely based on kinematics. We have compared the results obtained for TrES-1 with those for the other planet hosts listed in Table 4 and with a large comparison sample of 639 field stars taken from the catalog compiled by Soubiran & Girard (2005). In order to calculate the likelihood of any given object to belong to either of the two populations on the basis of its galactic kinematics, a number of approaches can be adopted. We elect to carry out population assignments using the classifications by Mishenina et al. (2004), Bensby

et al. (2003, 2005), Venn et al. (2004), and Brewer & Carney (2005). Mishenina et al. (2004) adopt a classification scheme based on the assumption of a Gaussian velocity ellipsoid for the thin and thick disk populations, with kinematical parameters (velocity dispersion and asymmetric drift) taken from Soubiran et al. (2003), and relative densities of the two populations of 75% and 25%, respectively. The approach of Bensby et al. (2003, 2005) is similar in principle, although the authors used the thick-disk-to-thin-disk probability ratio TD/D, a slightly different velocity ellipsoid, and the observed fractions of each population in the solar neighborhood (4% and 96%, respectively). Finally, Venn et al. (2004) and Brewer & Carney (2005) employ a standard Bayesian classification scheme assuming a Gaussian velocity ellipsoid with components from Dehnen & Binney (1998) and Soubiran et al. (2003), and uniform prior probability distributions for both populations. In columns 11 through 17 of Table 4 we report the membership probabilities for TrES-1 and the sample of stars with planets computed with the methods described above, plus a population assignment based on Venn's scheme but using the Bensby et al. (2003) values for the prior probability distributions.

As a consistency check between the various methods, let us first consider objects classified as very likely thick disk members by the different methods. According to the Mishenina et al. (2004) approach, five planet-bearing stars (HD 13445, HD 47536, HD 111232, HD 114762, and HD 195019A) have $P^{\rm thick} \geq 0.90$. Bensby et al. (2003) classify as thick disk members objects with $TD/D \geq 10$ (i.e., objects which are ten times more likely of being thick disk rather than thin disk members). With this prescription, the second classification scheme assigns to the thick disk only HD 47536 and HD 114762, a K0III giant and the lowest-metallicity object known to-date to harbor a planetary mass object and a well-known member of the thick-disk population, respectively. The Bayesian approach of Venn et al. (2004) with the Bensby et al. (2003) prior probability distributions classifies the same two stars as thick disk members with $P_2^{\rm thick} \geq 0.90$. According to these last two schemes, HD 13445, HD 111232, and HD 195019A all have intermediate kinematics, with $TD/D \simeq 2-3$ and $P_2^{\rm thick} \simeq 0.60$, although the thick disk membership is still more probable, albeit without high confidence. Finally, if uniform priors are used, $P_1^{\rm thick} \geq 0.90$ for 10 objects, a sample including all the five stars with $P^{\rm thick} \geq 0.90$, plus HD 27894, HD 88133, HD 114729, HD 190360, and HD 330075. These objects all have $P^{\rm thick} \geq 0.85$, $TD/D > 1$, and $P_2^{\rm thick} = 0.50$, with the exception of HD 114729, for which $TD/D = 0.65$, and HD 190360, for which $P^{\rm thick} = 0.63$ and $P_2^{\rm thick} = 0.40$. Then, we can state as a general conclusion that all the purely kinematic indicators agree to a significant extent, and the very likely thick disk members, with extreme kinematics, are all readily identified, regardless of the classification scheme. In this context, TrES-1 appears to be a very likely member of the thin disk population, with $P^{\rm thin} = 0.92$, $TD/D = 0.02$, $P_1^{\rm thin} = 0.70$, and $P_2^{\rm thin} = 1.0$.

Finally, in Figure 10 we show the Toomre diagram $UW - V$ ($UW = \sqrt{U^2 + W^2}$) for the Soubiran & Girard (2005) and the planet host samples (left and right panel, respectively). TrES-1 is indicated with a large filled black dot. In the two panels of Figure 10, symbols of different shapes indicate objects with $P^{\rm thin} \geq 0.90$ and $P^{\rm thick} \geq 0.90$. For the planet hosts sample we also plot objects with intermediate kinematics. In addition, the solid lines identify regions of constant peculiar space velocities $v_{\rm p} = \sqrt{U^2 + V^2 + W^2}$, with $v_{\rm p} = 85$ km s^{-1} and $v_{\rm p} = 180$ km s^{-1}, respectively, which is the simple recipe proposed by Feltzing et al. (2003) and Nissen (2004) to operationally distinguish between thick and thin disk populations. By inspection of Figure 10, we see how, in both cases, the two classification schemes select basically the same clean samples of stars in the two kinematic populations. Also, many of the stars with planets assigned to either the thick or thin disk populations with lower confidence appear to be borderline cases, according to the simple criterion based on $v_{\rm p}$. Again, a comparison between the two different classification schemes results in very broad agreement. And again, simply based on its value of $v_{\rm p}$, TrES-1 is confidently assigned to the thin disk population.

4.2. Hybrid Indicators

In Figure 11 the distribution of the X parameter defined by Schuster et al. (1993) is shown, for the comparison sample of field stars (solid histogram), the planet hosts (dashed-dotted histogram), and TrES-1 (solid arrow). The X parameter is a linear combination of $V_{\rm rot}$ and [Fe/H], where $V_{\rm rot} = V + 220$ km s^{-1} (corrected for the rotation velocity of the LSR). All the X values are also listed for the planet hosts sample in column 18 of Table 4.

According to Schuster et al. (1993) and Karataş et al. (2005), values of $-21 < X < -6$ identify a clean sample of thick disk stars. Within the context of this scheme, 94 stars are assigned to the thick disk with minimal contamination. On the other hand, 47 of the 70 field stars with $P^{\rm thick} \geq 0.90$, and 46 out of 66 objects with both $P^{\rm thick} \geq 0.90$ *and* $85 \leq v_{\rm p} \leq 180$ km s^{-1} fall in this range. As for what concerns the sample of stars with planets, five objects (HD 6434, HD 47536, HD 111232, HD 114729, and HD 114762) have $-21 < X < -6$. These include two assigned to the thick disk by all other criteria (HD 47536 and HD 114762), two low-confidence thick disk members (HD 111232, HD 114729), and one star (HD 6434) for which the other criteria give mixed results. The hybrid method thus appears to perform slightly more poorly with respect to both those based on the determination of membership probabilities and on the values of peculiar velocities, but its accuracy appears nonetheless comparable. Finally, objects with $X \lesssim -33$ are assigned with high confidence to the thin disk, according to Schuster et al. (1993) and Karataş et al. (2005). The arrow at $X \simeq -33$

identifies TrES-1, which is thus confirmed as a likely member of the thin disk also on the basis of the X indicator.

4.3. Chemical Indicators

Recent studies (e.g., Bensby et al. 2003, 2005; Brewer & Carney 2005. See Nissen 2004, and references therein, for a review of the subject) have highlighted how the thin and thick disk of the Milky Way Galaxy appear to overlap significantly in metallicity, when [Fe/H] is utilized as a reference, while they are separated in [α/Fe] abundances. The variations in the abundances in α-elements can then be used to not only explain the history of star-formation processes in the Galaxy (as it is usually done), but also to identify and understand systematic differences in the chemical composition of the thin and thick disk.

It is customary to use averages of α-element abundances for a variety of studies of chemical abundance trends in the Milky Way Galaxy and beyond (e.g., Venn et al. 2004, and references therein). Usually, elements with similar trends are considered. For the purpose of this analysis, we have utilized [α/Fe] defined as $\frac{1}{4}$([Mg/Fe]+[Si/Fe]+[Ca/Fe]+[Ti/Fe]). One could in principle adopt other combinations, and include other α-elements such as O and S. We have chosen to not consider these elements in our discussion for a number of reasons. First, as already mentioned in Section 2.1 and Section 3.2, the sulfur lines and the UV OH lines are outside the wavelength domain of our Keck/HIRES and HET/HRS spectra. Second, the forbidden [OI] lines at 6300 Å and 6363 Å are too weak to be measured reliably in dwarf stars such as TrES-1. Third, the oxygen triplet lines near 7770 Å have very high excitation levels (9.15 eV), thus the sensitivity to non-LTE effects is significantly greater than in the case of the much lower excitation potential lines of Mg, Si, Ca, and Ti. Finally, there is significant disagreement in the literature on abundance trends of both oxygen and sulfur (e.g, Nissen et al. 2002; Jonsell et al. 2005; Caffau et al. 2005). In the case of oxygen, for example, typical discrepancies of 0.1-0.2 dex are found when [OI] and oxygen triplet abundances are compared (e.g., Ecuvillon et al. 2005a).

We show in Figure 12 the [α/Fe] vs. [Fe/H] diagram for 425 stars in the catalog of Soubiran & Girard (2005) and for 78 stars with planets and 41 comparison field stars for which a value of [α/Fe] could be derived from the Bodaghee et al. (2003) and Beirão et al. (2005) samples (left and right panels, respectively). TrES-1 is indicated by the large filled dot, as before. In the left panel, crosses are thick disk stars and open circles are thin disk objects, based on the purely kinematic criterion of Mishenina et al. (2004) described above. While there is a significant overlap in metallicity, the separation between the two populations is clear when considering metal-poor objects ([Fe/H] < -0.5) with large values

(> 0.2) of [α/Fe] abundances. Again, based on a purely chemistry-based indicator, TrES-1 appears to belong clearly to the thin disk. In the right panel, the same plot for the planet-harboring stars and the control sample closely follows the same trend. One of the two objects assigned to the thick disk by all the classification schemes discussed before (HD 114762) is also among those with the largest values of [α/Fe] (as it can be seen by looking at the last column of Table 4, in which all the [α/Fe] abundances for planet hosts are reported), while no measurement is available for the other thick disk star (HD 47536). Two other objects (HD 6434 and HD 37124) with [α/Fe]$\sim 0.15 - 0.20$ have intermediate kinematics. As a further confirmation, the three planet hosts are the most metal-poor objects in the sample studied here.

However, a visual comparison between the two panels in Figure 12 shows evidence of an interesting feature. The metal-rich sample ([Fe/H]> 0.0) of planet hosts appears to be systematically less abundant in [α/Fe] than the large sample of field stars from Soubiran & Girard (2005), by ~ 0.1 dex. In order to make a more meaningful statement on the reality of this difference, we first show in Figure 13 a comparison between the [α/Fe] values for all stars in the Soubiran & Girard (2005) sample, the planet hosts and comparison field stars from Bodaghee et al. (2003) and Beirão et al. (2005), and TrES-1, expressed as a function of [Fe/H] and $T_{\rm eff}$, respectively. No clear trend with temperature is apparent: Stars with planets have lower [α/Fe]-values than planetless field stars for a broad range of $T_{\rm eff}$, although slightly less so at the cooler side. On the other hand, the trend with metallicity does appear significant. We summarize in Table 5 the results of a series of Kolmogorov-Smirnov (K-S) tests we have run to measure to what extent the [α/Fe] distributions for the three samples might differ one from the other, and expressed in terms of the probability $Pr(D)$ of the null hypothesis (i.e. that the distributions are the same). We have done so by considering the [α/Fe] abundances for all values of [Fe/H], and by restricting the comparison to [α/Fe] values in the two regimes [Fe/H]≤ 0.0 and [Fe/H]> 0.0. Indeed, the [α/Fe] distributions for the Soubiran & Girard (2005) sample and for the control sample of field stars of Bodaghee et al. (2003) and Beirão et al. (2005) appear globally indistinguishable, and this holds true when the two samples are compared in different metallicity bins. However, the [α/Fe] distribution for the planet hosts sample appears to differ significantly from both the other cases, when no restriction on [Fe/H] is imposed. The distribution of [α/Fe] values for the planet hosts is significantly different from that of the stars in the large catalog of Soubiran & Girard (2005) when different [Fe/H] ranges are considered, but less so for the [Fe/H]≤ 0.0 bin. This confirms the conclusions drawn from the comparison presented in Figure 13. Stars with planets and the smaller control sample appear instead to have the same distribution in the metal-poor regime, while they exhibit somewhat significant differences in the metal-rich regime.

Assuming the difference is real, what is a likely cause for its existence? One possible reason could be systematics. For instance, inhomogeneous $T_{\rm eff}$ scales determinations using different methods of spectroscopic analyses are a likely outcome, and systematic differences in this critical parameter translate in systematic differences in [Fe/H] and thus in any elemental abundance [X/Fe]. Some of the planet hosts and the stars in the control sample of Bodaghee et al. (2003) and Beirão et al. (2005), 22 and 25 respectively, are in common with the Soubiran & Girard (2005) sample, thus the values of [α/Fe] obtained in the two cases can be directly compared. In the two upper panels of Figure 14 we show the comparison between the $T_{\rm eff}$ and [Fe/H] determinations for stars common to both studies. Average systematic differences in the two cases amount to $\Delta T_{\rm eff} \approx 50 - 60$ K and Δ[Fe/H]≈ 0.03 dex. A mild dependence of the differences between the α-element abundances Δ[α/Fe] on $T_{\rm eff}$ is found, but less so on [Fe/H], as shown in the two bottom panels of Figure 14. In all cases, the trend for planet hosts is closely traced by the control sample, and systematic differences of the same magnitude appear to be present whether one compares stars with planets or control sample field stars in common to both studies. On average, stars with planets and comparison field stars in common with the two studies appear to differ by ~ 0.06 dex and ~ 0.04 dex in [α/Fe], respectively.

In light of this, intriguing as it might be, one could simply interpret the observed signature in Figure 13 in terms of unknown systematics in the abundance determination procedures adopted by the different authors. However, if systematics were to be the dominant effect, then one would not expect to find significant differences in the two samples analyzed in a uniform manner by the same authors, as instead the K-S test analysis seems to indicate. While on the one hand the discrepancies between the two samples of Bodaghee et al. (2003) and Beirão et al. (2005) could still be in part explained invoking small-number statistics and selection effects (e.g., too few metal-rich stars in their control sample), on the other hand the possibility that the observed feature is not an artifact due to systematics might not be discarded completely.

To put this point under further scrutiny, we have investigated whether age might be a factor in the equation. For example, if the sub-sample of metal-rich planet hosts is systematically composed of young objects, which are more likely to have their chemical composition dominated by heavy-element materials from Type Ia supernovae, this might in turn contribute to explain the underabundance in [α/Fe]. We present in the two panels of Figure 15 the age-metallicity diagram and a plot of [α/Fe] vs. age for stars in the Soubiran & Girard (2005) catalog, for TrES-1, and for the stars with planets and the control sample of field stars from Bodaghee et al. (2003) and Beirão et al. (2005). Stellar age estimates were obtained from the Nordström et al. (2004) catalog, except for TrES-1, for which the preliminary estimate by Sozzetti et al. (2004) was used. As one can see, stars with planets do not appear to

be particularly younger than planetless field stars at any given metallicity, and the former sample seems underabundant in [α/Fe] at all ages. Thus, one would tend to exclude age as primary responsible for the feature observed in Figure 13.

A large number of spectroscopic studies of stars with planets and control samples have been undertaken in the past (see the Introduction Section), yet none have noticed the apparent deficiency of [α/Fe] among the former relative to the latter. There are three possible reasons why we have discerned the effect while others have not. First, the magnitude of the effect is small, and few workers have averaged the results from several elements. As long as the elements have similar sensitivities to systematic effects such as temperature and gravity, using four elements rather than one has an obvious advantage. Second, a number of studies have not employed large enough numbers of the two classes of stars. Finally, some studies may have been vulnerable to systematic differences in the analysis procedures between differing datasets. An extensive review of all such prior comparisons is beyond the scope of this paper, but we hope that future work will indeed consider these four α-elements both individually and jointly.

While on the basis of the evidence presented here no definite conclusion can be drawn, the possible existence of an underabundance in [α/Fe] in stars with planets with respect to non-planet hosts is nevertheless intriguing and worthy of further investigation, to ascertain its reality or to firmly rule it out on the basis of e.g. the presence of identifiable systematics.

5. Concluding Remarks

In this work we have carried out an abundance analysis of 16 elements for the parent star of the transiting extrasolar planet TrES-1. The resulting average abundance of $< [X/\mathrm{H}] >= -0.02 \pm 0.06$ is in good agreement with initial estimates of solar metallicity based on iron (Sozzetti et al. 2004; Laughlin et al. 2005). TrES-1 appears not to be chemically peculiar in any measurable way when compared to a large sample of known stars with planets. No convincing evidence for statistically significant trends of metallicity [X/H] with condensation temperature T_c can be found for TrES-1 or other planet hosts, a further indication that selective accretion of planetary material is not likely to be responsible for the observed high metal content of stars with detected planets, a conclusion similar to those drawn by others (e.g., Santos et al. 2001, 2004a; Fischer & Valenti 2005). Using its abundance and kinematic information, we have classified TrES-1 as a likely member of the thin disk population, and provided updated membership probabilities for a large set of planet hosts, based on the relative agreement between different statistical indicators (purely kinematic in nature, solely based on chemistry, and a combination of the two). Finally, we have highlighted an apparent

systematic underabundance in [α/Fe] of stars with planets compared to a large comparison sample of field stars. The more likely cause for this signature resides in unknown systematics in the details of the abundance analysis procedures adopted by different authors. However, we have found hints for differences between the [α/Fe] abundances of planet hosts and control samples analyzed in exactly the same way. In this respect, we stress the importance of continuously updating and expanding uniform, detailed studies of the chemical composition of planet hosts (including both refractory and volatile elements spanning a wide range of condensation temperatures) as new objects are added to the list, as well as statistically significant control samples of stars without any detected planets, following those recently undertaken by e.g., Bodaghee et al. (2003), Santos et al. (2004a, 2004b, 2005), Israelian et al. (2004), Ecuvillon et al. (2004a, 2004b, 2005a, 2005b, 2005c), Beirão et al. (2005), Gilli et al. (2005), Fischer & Valenti (2005), Valenti & Fischer (2005), and Gonzalez (2005). Such investigations would also help to disentangle possible signatures induced by the presence of planets from effects related instead to Galactic chemical evolution.

A.S. acknowledges support from the Keck PI Data Analysis Fund (JPL 1262605). G.T. acknowledges partial support for this work from NASA Origins grant NNG04LG89G. J.L. is partially supported by an NSF grant AST-0307340. It is a pleasure to thank C. Allende Prieto for stimulating discussions. An anonymous referee provided very useful suggestions and comments. Some of the data presented herein were obtained at the Hobby-Eberly Telescope, which is operated by the McDonald Observatory on behalf of the University of Texas at Austin, the Pennsylvania State University, Stanford University, Ludwig Maximillians Universität München, and Georg August Universität Göttingen. The other data were obtained at the W.M. Keck Observatory, which is operated as a scientific partnership among the California Institute of Technology, the University of California and the National Aeronautics and Space Administration. The Observatory was made possible by the generous financial support of the W.M. Keck Foundation. The authors wish to recognize and acknowledge the very significant cultural role and reverence that the summit of Mauna Kea has always had within the indigenous Hawaiian community. Without their generous hospitality, the Keck observations presented here would not have been possible. This research has made use of NASA's Astrophysics Data System Abstract Service and of the SIMBAD database, operated at CDS, Strasbourg, France.

REFERENCES

Alonso, R., et al. 2004, ApJ, 613, L153

Anders, E., & Grevesse, N. 1989, GeCoA, 53, 197

Barbieri, M., & Gratton, R. G. 2002, A&A, 384, 879

Beirão, P., Santos, N. C., Israelian, G., & Mayor, M., 2005, A&A, 438, 251

Bensby, T., Feltzing, S., & Lundström, I. 2003, A&A, 410, 527

Bensby, T., Feltzing, S., Lundström, I., & Ilyin, I. 2005, A&A, 433, 185

Biémont, E., Baudoux, M., Kurucz, R. L., Ansbacher, W., & Pinnington, E. H. 1991, A&A, 249, 539

Blackwell, D. E., Shallis, M. J., & Simmons, G. J. 1982, MNRAS, 199, 21

Blackwell, D. E., Menon, S. L. R., & Petford, A. D. 1983, MNRAS, 204, 883

Blackwell, D. E., Booth, A. J., Menon, S. L. R., & Petford, A. D. 1986, MNRAS, 220, 289

Bodaghee, A., Santos, N. C., Israelian, G., & Mayor, M. 2003, A&A, 404, 715

Boesgaard, A. M., & King, J. R. 2002, ApJ, 565, 587

Boss, A. P. 2002, ApJ, 567, L149

Brewer, M.-M., & Carney, B. W. 2005, AJ, accepted (astro-ph/0509267)

Caffau, E., Bonifacio, P., Faraggiana, R., Francois, P., Gratton, R. G., & Barbieri, M. 2005, A&A, 441, 533

Carney, B. W., Latham, D. W., & Laird, J. B. 1989, AJ, 97, 423

Charbonneau, D. 2004, in Scientific Frontiers in Research on Extrasolar Planets, D. Deming & S. Seager eds., ASP Conf. Ser., 294, 449

Chen, Y. Q., Nissen, P. E., Zhao, G., Zhang, H. W., & Benoni, T. 2000, A&AS, 141, 491

Chen, Y. Q., Nissen, P. E., & Zhao, G. 2004, A&A, 425, 697

Cody, A. M., & Sasselov, D. D. 2005, ApJ, 704, 713

Dehnen, W., & Binney, J. J. 1998, MNRAS, 298, 387

Deliyannis, C. P., Cunha, K., King, J. R., & Boesgaard, A. M. 2000, AJ, 119, 2437

Dotter, A., & Chaboyer, B. 2003, ApJ, 596, L101

Ecuvillon, A., Israelian, G., Santos, N. C., Mayor, M., García López, R. J., & Randich, S. 2004a, A&A, 418, 703

Ecuvillon, A., Israelian, G., Santos, N. C., Mayor, M., Villar, V., & Bihain, G. 2004b, A&A, 426, 619

Ecuvillon, A., Israelian, G., Santos, N. C., Shchukina, N. G., Mayor, M., & Rebolo, R. 2005a, A&A, in press (astro-ph/0509326)

Ecuvillon, A., Israelian, G., Santos, N. C., Mayor, M., & Gilli, G. 2005b, to appear in the proceedings of Haute Provence Observatory Colloquium '10th anniversary of 51Peg-b: status of and prospects for hot Jupiter studies' (astro-ph/0509494)

Ecuvillon, A., Israelian, G., Santos, N. C., Mayor, M., & Gilli, G. 2005c, A&A, accepted (astro-ph/0512221)

Edvardsson, B., Andersen, J., Gustafsson, B., Lambert, D. L., Nissen, P. E., & Tomkin, J. 1993, A&A, 275, 101

Feltzing, S., & Gustafsson, B. 1998, A&AS, 129, 237

Feltzing, S., Bensby, T., & Lundström, I. 2003, A&A, 397, L1

Fischer, D. A., & Valenti, J. 2005, ApJ, 622, 1102

Fuhrmann, K., Pfeiffer, M. J., & Bernkopf, J. 1997, A&A, 326, 1081

Fuhrmann, K., Pfeiffer, M. J., & Bernkopf, J. 1998, A&A, 336, 942

García López, R. J., & Pérez de Taoro, M. R. 1998, A&A, 334, 599

Garz, T. 1973, A&A, 26, 471

Gilli, G., Israelian, G., Ecuvillon, A., Santos, N. C., & Mayor, M. 2005, A&A, accepted (astro-ph/0512219)

Gilmore, G., & Reid, N. 1983, MNRAS, 202, 1025

Giménez, A. 2000, A&A, 356, 213

Gonzalez, G. 1997, MNRAS, 285, 403

Gonzalez, G. 1998a, A&A, 334, 221

Gonzalez, G. 1998b, in Brown Dwarfs and Extrasolar Planets, R. Rebolo, E.L. Martin & M.R. Zapatero Osorio eds., ASP Conf. Ser., 134, 431

Gonzalez, G., & Vanture, A. D. 1998, A&A, 339, L29

Gonzalez, G. 1999, MNRAS, 308, 447

Gonzalez, G., & Laws, C. 2000, AJ, 119, 390

Gonzalez, G., Laws, C., Tyagi, S., & Reddy, B. E. 2001, AJ, 121, 432

Gonzalez, G. 2003, Rev. Mod. Phys., 75, 101

Gonzalez, G. 2005, MNRAS, accepted (astro-ph/0512222)

Heiter, U., & Luck, R. E. 2003, AJ, 126, 2015

Grevesse, N., & Sauval, A. J. 1998, Space Sci. Rev., 85, 161

Horne, K. 2004, ASP Conf. Ser. 294: Scientific Frontiers in Research on Extrasolar Planets, eds. D. Deming & S. Seager, 361

Huang, C., Zhao, G., Zhang, H. W., & Chen, Y. Q. 2005, MNRAS, 363, 71

Ida, S., & Lin, D. N. C. 2005, ApJ, 626, 1045

Israelian, G., Santos, N. C., Mayor, M., & Rebolo, R. 2001, Nature, 411, 163

Israelian, G., Santos, N. C., Mayor, M., & Rebolo, R. 2003, A&A, 405, 753

Israelian, G., Santos, N. C., Mayor, M., & Rebolo, R. 2004, A&A, 414, 601

Jonsell, K., Edvardsson, B., Gustafsson, B., Magain, P., Nissen, P. E., & Asplund, M. 2005, A&A, 440, 321

Karataş, Y., Bilir, S., & Schuster, W. J. 2005, MNRAS, 360, 1345

Kornet, K., Bodenheimer, P., Rózyczka, M., & Stepinski, T. F. 2005, A&A, 430, 1133

Kurucz, R. L. 1993, ATLAS9 Stellar Atmosphere Programs and 2 km/s Grid CDROM, Vol. 13, Smithsonian Astrophysical Observatory

Kurucz, R., & Bell, B. 1995, Atomic Line Data (R.L. Kurucz and B. Bell) Kurucz CD-ROM No. 23. Cambridge, Mass.: Smithsonian Astrophysical Observatory, 1995, 23

Laughlin, G. & Adams, F. C. 1997, ApJ, 491, L51

Laughlin, G. 2000, ApJ, 545, 1064

Laughlin, G., Wolf, A., Vanmunster, T., Bodenheimer, P., Fischer, D., Marcy, G. W., Butler, R. P., & Vogt, S. S. 2005, ApJ, 621, 1072

Laws, C., & Gonzalez, G. 2001, ApJ, 553, 405

Laws, C., Gonzalez, G., Walker, K. M., Tyagi, S., Dodsworth, J., Snider, K., & Suntzeff, N. B. 2003, AJ, 125, 2664

Lee, J.-W., & Carney, B. W. 2002, AJ, 124, 1511

Lodders, K. 2003, ApJ, 591, 1220

Majewski, S. R. 1993, ARA&A, 31, 575

Mandell, A. M., Ge, J., & Murray, N. 2004, AJ, 127, 1147

Martell, S., & Laughlin, G. 2002, ApJ, 577, L45

Mihalas, D., & Binney, J. 1981, Galactic astronomy: Structure and kinematics - 2nd edition (San Francisco, CA, W. H. Freeman and Co.)

Mishenina, T. V., Kovtyukh, V. V., Soubiran, C., Travaglio, C., & Busso, M. 2002, A&A, 396, 189

Mishenina, T. V., Soubiran, C., Kovtyukh, V. V., & Korotin, S. A. 2004, A&A, 418, 551

Monet, D. G., et al. 2003, AJ, 125, 984

Montalbán, J., & Rebolo, R. 2002, A&A, 386, 1039

Murray, N., & Chaboyer, B. 2002, ApJ, 566, 442

Neuforge-Verheecke, C., & Magain, P. 1997, A&A, 328, 261

Nissen, P. E., Primas, F., Asplund, M., & Lambert, D. L. 2002, A&A, 390, 235

Nissen, P. E. 2004, in Origin and Evolution of the Elements, A. McWilliam and M. Rauch eds., Cambridge University Press: Carnegie Observatories Astrophysics Series., 156

Nissen, P. E., Chen, Y. Q., Asplund, M., & Pettini, M. 2004, A&A, 415, 993

Nordström, B., et al. 2004, A&A, 418, 989

Paulson, D. B., Sneden, C., & Cochran, W. D. 2003, AJ, 125, 3185

Pepe, F., et al. 2004, A&A, 423, 385

Pinsonneault, M. H., DePoy, D. L., & Coffee, M. 2001, ApJ, 556, L59

Prochaska, J. X., Naumov, S. O., Carney, B. W., McWilliam, A., & Wolfe, A. M. 2000, AJ, 120, 2513

Prochaska, J. X., & Wolfe, A. M. 2000, ApJS, 121, 369

Queloz, D., et al. 2000a, A&A, 354, 99

Ramírez, S. V. & Cohen, J. G. 2002, AJ, 123, 3277

Reddy, B. E., Lambert, D. L., Laws, C., Gonzalez, G., & Covey, K. 2002, MNRAS, 335, 1005

Reddy, B. E., Tomkin, J., Lambert, D. L., & Allende Prieto, C. 2003, MNRAS, 340, 304

Reid, I. N. 2002, PASP, 114, 306

Ryan, S. 2000, MNRAS, 316, L35

Sadakane, K., Ohkubo, M., Takeda, Y., Sato, B., Kambe, E., & Aoki, W. 2002, PASJ, 54, 911

Sandquist, E. L., Dokter, J. J., Lin, D. N. C., & Mardling, R. A. 2002, ApJ, 572, 1012

Santos, N. C., Israelian, G., & Mayor, M. 2000, A&A, 363, 228

Santos, N. C., Israelian, G., & Mayor, M. 2001, A&A, 373, 1019

Santos, N. C., García López, R. J., Israelian, G., Mayor, M., Rebolo, R., García-Gil, A., Pérez de Taoro, M. R, & Randich, S. 2002, A&A, 386, 1028

Santos, N. C., Israelian, G., Mayor, M., Rebolo, R., & Udry, S. 2003, A&A, 398, 363

Santos, N. C., Israelian, G., & Mayor, M. 2004a, A&A, 415, 1153

Santos, N. C., et al. 2004b, A&A, 427, 1085

Santos, N. C., Israelian, G., Mayor, M., Bento, J. P., Almeida, P. C., Sousa, S. G., & Ecuvillon, A. 2005, A&A, 437, 1127

Savanov, I. S., Huovelin, J., & Tuominen, I. 1990, A&AS, 86, 531

Schuster, W. J., Parrao, L., & Contreras Martínez, M. E. 1993, A&AS, 97, 951

Simmerer, J., Sneden, C., Ivans, I. I., Kraft, R. P., Shetrone, M. D., & Smith, V. V. 2003, AJ, 125, 2018

Smith, G., & Raggett, D. S. J. 1981, Journal of Physics B Atomic Molecular Physics, 14, 4015

Smith, G. 1988, Journal of Physics B Atomic Molecular Physics, 21, 2827

Smith, V. V., Cunha, K., & Lazzaro, D. 2001, AJ, 121, 3207

Sneden, C. A. 1973, Ph.D. Thesis, The University of Texas at Austin

Sneden, C. A., Gratton, R. G., & Crocker, D. A 1991, A&A, 246, 354

Sozzetti, A. 2004, MNRAS, 354, 1194

Sozzetti., A., et al. 2004, ApJ, 616, L167

Soubiran, C., Bienaymé, O., & Siebert, A. 2003, A&A, 398, 141

Soubiran, C., & Girard, P. 2005, A&A, 438, 139

Takeda, Y., et al. 2001, PASJ, 53, 1211

Thévenin, F., & Idiart, T. P. 1999, ApJ, 521, 753

Thorén, P., & Feltzing, S. 2000, A&A, 363, 692

Valenti, J. A., & Fischer, D. A. 2005, ApJS, 159, 141

Vauclair, S. 2004, ApJ, 605, 874

Venn, K. A., Irwin, M., Shetrone, M. D., Tout, C. A., Hill, V., & Tolstoy, E. 2004, AJ, 128, 1177

Yong, D., Lambert, D. L., Allende Prieto, C., & Paulson, D. B. 2004, ApJ, 603, 697

Zhao, G., Chen, Y. Q., Qiu, H. M., & Li, Z. W. 2002, AJ, 124, 2224

This preprint was prepared with the AAS LaTeX macros v5.2.

Fig. 1.— Top panel: a 5Å region in the observed spectrum (dots) of TrES-1 containing two Al I lines (6696.0Å and 6698.7Å) used in the analysis. Superposed are three spectral syntheses for different values of [Al/Fe]. Bottom panel: same as top panel, but for a 3Å region containing the Zn I line at 4722.2Å.

Fig. 2.— Chemical abundances $[X/\mathrm{H}]$ measured in TrES-1 as a function of element number Z. Error bars correspond to the error of the mean $\sigma/\sqrt{n}$. The average solar abundance ratio $<[X/\mathrm{H}]>= 0.0$ is indicated by a horizontal dashed line. The solid line is the average abundance ratio determined for TrES-1 ($<[X/\mathrm{H}]>\simeq -0.02$).

Fig. 3.— $[X/\mathrm{H}]$ versus [Fe/H] for 8 elements measured in TrES-1 (filled black circle) and in comparison samples of planet hosts (open circles). The literature sources for the comparison samples are the following. [V/H], [Cr/H], [Mn/H], [Co/H], [Ni/H], [Si/H], [Ca/H], and [Sc/H]: Bodaghee et al. 2003.

Fig. 4.— Same as Figure 3, but for the remaining 8 elements that could be measured in TrES-1. The literature sources for the comparison samples are the following. [Ti/H]: Bodaghee et al. 2003; [Na/H], [Mg/H], and [Al/H]: Beirão et al. 2005; [Cu/H] and [Zn/H]: Ecuvillon et al. 2004b; [Ba/H]: Sadakane et al. 2002 and 86; [Y/H]: Sadakane et al. 2002.

Fig. 5.— Lithium abundance $\log \epsilon(\mathrm{Li})$ as a function of effective temperature $T_{\rm eff}$ for planet hosts. The black filled circle corresponds to TrES-1, while open circles are Lithium measurements for the sample of stars with planets analyzed by Israelian et al. (2004). Arrows indicate that only upper limits on $\log \epsilon(\mathrm{Li})$ are available.

Fig. 6.— Chemical abundances $[X/\mathrm{H}]$ measured in TrES-1 versus condensation temperature T_c (taken from Lodders (2003)). A linear least square fit to the data in the form $[X/\mathrm{H}] = \mathrm{a} + \mathrm{b}T_c$ (solid line) provides no evidence of a measurable trend of abundance with condensation temperature.

Fig. 7.— Differences Δ[Fe/H] between the iron abundances derived by Santos et al. (2004a) (S04) and those obtained by Santos et al. (2000, 2001, 2003). The average difference (dotted line) is null, with a standard deviation of ~ 0.03 dex. No trend is visible as a function [Fe/H] (a rank-correlation test gave a probability of no correlation $p = 0.84$).

Fig. 8.— Slopes of the $[X/\mathrm{H}]$-T_c relation as a function of [Fe/H] for TrES-1 (this work, filled black circle) and for a sample of planet hosts (filled black circles) and comparison field stars (open triangles) uniformly studied by Bodaghee et al. (2003), Ecuvillon et al. (2004a, 2004b, 2005a), and Beirão et al. (2005).

Fig. 9.— Slopes of the $[X/H]$-T_c relation as a function of $T_{\rm eff}$ for TrES-1 (this work, filled black circle) and for a sample of planet hosts (filled black circles) and comparison field stars (open squares) uniformly studied by Bodaghee et al. (2003), Ecuvillon et al. (2004a, 2004b,2005a), and Beirão et al. (2005).

Fig. 10.— Left: Toomre diagram for the Soubiran & Girard (2005) stellar sample. Solid lines identify regions of constant peculiar velocity $v_{\rm p,1} = 85$ km s^{-1} and $v_{\rm p,2} = 180$ km s^{-1}, respectively. Objects with $v_{\rm p} < v_{\rm p,1}$ are thin disk stars, while those with $v_{\rm p,1} < v_{\rm p} < v_{\rm p,2}$ are assigned to the thick disk population. Asterisks and triangles are likely members of the thin and thick disk, respectively, according to the Mishenina et al. (2004) kinematic classification. Crosses identify stars with intermediate kinematics. The large filled dot represents TrES-1. Right: The same diagram, but for TrES-1 and a large sample of planet hosts. Squares are objects with $P^{\rm thin} \geq 0.90$, asterisks are stars with $P^{\rm thick} \geq 0.90$, and crosses identify objects with intermediate kinematics.

Fig. 11.— Distributions of the X indicator, defined by Schuster et al. (1993), for the Soubiran & Girard (2005) sample (solid histogram) and for a sample of planet hosts (dashed-dotted histogram). The solid arrow corresponds to the X value for TrES-1.

Fig. 12.— Left: $[\alpha/Fe]$ vs. [Fe/H] for the Soubiran & Girard (2005) sample. Open circles have $P^{\rm thin} \geq 0.90$, while crosses are stars with $P^{\rm thick} \geq 0.90$. Stars with intermediate kinematics are not shown. TrES-1 is identified by the filled black dot. Right: the same diagram for a sample of planet hosts (open circles) and comparison field stars (crosses) studied by Bodaghee et al. (2003) and Beirão et al. (2005).

Fig. 13.— Left: same as Figure 12, but now comparing all stars in the Soubiran & Girard (2005) catalog (filled black circles) with TrES-1 (this work, green circle), planet hosts (green circles) and comparison field stars (red circles) from Bodaghee et al. (2003) and Beirão et al. (2005). Right: the same comparison, in the $[\alpha/Fe]$-$T_{\rm eff}$ plane.

Fig. 14.— Top panels: differences in $T_{\rm eff}$ and [Fe/H] values for a sample of planet hosts (filled dots) and stars without known planets (open squares) in common with the Soubiran & Girard (2005) and the Bodaghee et al. (2003) and Beirão et al. (2005) samples. Bottom panels: differences $[\alpha/Fe]_1 - [\alpha/Fe]_2$ between the former and the latter α-element abundances as a function of $T_{\rm eff}$ and [Fe/H]. Solid lines indicate a linear fit to the data.

Fig. 15.— Left: a comparison, in the age-metallicity diagram, between stars in the Soubiran & Girard (2005) catalog, TrES-1 (this work), and planet hosts and comparison field stars from Bodaghee et al. (2003) and Beirão et al. (2005). The legend for the symbols is the same as in Figure 13. Right: the same comparion in the age-$[\alpha/Fe]$ plane.

Table 1. TrES-1 equivalent widths

λ (Å)	Species	χ_l	$\log gf$	EW$_\lambda$ (mÅ)	References
6154.23	Na I (Z= 11; $\log \epsilon_\odot = 6.33$)	2.10	−1.57	60.6	1
6318.72	Mg I (Z= 12; $\log \epsilon_\odot = 7.58$)	5.11	−1.97	Synth[a]	2
6319.24	Mg I	5.11	−2.22	Synth[a]	2
6965.41	Mg I	5.75	−1.51	Synth[a]	3
6696.02	Al I (Z= 13; $\log \epsilon_\odot = 6.47$)	3.14	−1.34	Synth[a]	2
6698.67	Al I	3.14	−1.64	Synth[a]	2
5665.56	Si I (Z= 14; $\log \epsilon_\odot = 7.55$)	4.92	−2.04	47.0	4
5690.43	Si I	4.93	−1.87	49.6	4
6145.02	Si I	5.61	−1.48	38.7	1
5260.39	Ca I (Z= 20; $\log \epsilon_\odot = 6.36$)	2.52	−1.72	51.7	5
5867.56	Ca I	2.93	−1.57	48.3	6
6166.44	Ca I	2.52	−1.14	98.7	5
6455.60	Ca I	2.52	−1.29	81.7	5
5657.88	Sc II (Z= 21; $\log \epsilon_\odot = 3.17$)	1.51	−0.50	63.1	7
5669.04	Sc II	1.50	−1.10	31.2	7
6245.64	Sc II	1.51	−1.13	32.6	7
4562.64	Ti I (Z= 22; $\log \epsilon_\odot = 5.02$)	0.02	−2.60	40.3	8
4820.42	Ti I	1.50	−0.39	68.7	9
4926.16	Ti I	0.82	−2.11	25.9	10
5219.70	Ti I	0.02	−2.24	64.7	8
5426.26	Ti I	0.02	−2.95	30.3	8
5880.31	Ti I	1.05	−1.99	25.8	10
5903.33	Ti I	1.05	−2.09	20.9	10
5922.12	Ti I	1.05	−1.41	54.8	10
5941.75	Ti I	1.05	−1.45	48.2	1
6064.63	Ti I	1.05	−1.89	34.6	1
6126.22	Ti I	1.05	−1.37	57.0	10
6312.24	Ti I	1.46	−1.50	27.5	9
6554.22	Ti I	1.46	−1.02	50.0	9
6556.06	Ti I	1.44	−1.07	51.4	9
6599.11	Ti I	0.90	−2.03	35.2	10

Table 1—Continued

λ (Å)	Species	χ_l	$\log gf$	EW$_\lambda$ (mÅ)	References
4568.31	Ti II	1.22	−2.52	36.9	11
4583.44	Ti II	1.17	−2.77	28.7	11
4589.96	Ti II	1.24	−1.75	82.3	11
5336.81	Ti II	1.58	−1.70	66.6	11
5418.80	Ti II	1.58	−1.86	48.6	11
6090.22	V I (Z= 23; $\log \epsilon_\odot = 4.00$)	1.08	−0.06	78.4	7
6216.34	V I	0.28	−1.29	74.2	7
6251.82	V I	0.29	−1.34	60.7	7
6274.64	V I	0.27	−1.67	39.7	7
5238.96	Cr I (Z= 24; $\log \epsilon_\odot = 5.67$)	2.71	−1.51	33.3	12
5537.74	Mn I (Z= 25; $\log \epsilon_\odot = 5.39$)	2.19	−2.02	79.5	7
4602.00	Fe I (Z= 26; $\log \epsilon_\odot = 7.48$)	1.61	−3.15	98.5	13
4745.80	Fe I	3.65	−1.29	108.9	13
4788.75	Fe I	3.23	−1.78	86.5	13
4802.52	Fe I	4.60	−1.69	27.6	13
4802.88	Fe I	3.69	−1.53	78.1	13
4809.94	Fe I	3.57	−2.57	32.6	13
4961.91	Fe I	3.63	−2.33	41.3	13
5016.48	Fe I	4.25	−1.54	43.3	13
5242.49	Fe I	3.63	−1.03	110.3	13
5373.70	Fe I	4.47	−0.80	83.4	13
5379.57	Fe I	3.69	−1.54	81.5	13
5386.34	Fe I	4.15	−1.72	49.7	13
5417.04	Fe I	4.41	−1.45	49.9	13
5472.71	Fe I	4.21	−1.56	64.5	13
5538.52	Fe I	4.21	−1.55	52.2	13
5560.21	Fe I	4.43	−1.06	64.2	13
5577.03	Fe I	5.03	−1.47	17.1	13
5638.26	Fe I	4.22	−0.74	110.1	13
5679.03	Fe I	4.65	−0.70	86.8	13
5696.10	Fe I	4.55	−1.79	20.7	13

Table 1—Continued

λ (Å)	Species	χ_l	$\log gf$	EW$_\lambda$ (mÅ)	References
5741.85	Fe I	4.25	−1.65	45.5	13
5778.45	Fe I	2.59	−3.46	40.2	13
5809.22	Fe I	3.88	−1.55	78.5	13
5811.92	Fe I	4.14	−2.27	18.2	13
5855.09	Fe I	4.60	−1.55	30.0	13
5909.97	Fe I	3.21	−2.63	55.3	13
5956.69	Fe I	0.86	−4.61	80.2	13
6027.05	Fe I	4.07	−1.14	83.6	13
6151.62	Fe I	2.17	−3.30	69.3	13
6165.36	Fe I	4.14	−1.51	57.2	13
6265.13	Fe I	2.17	−2.55	114.4	13
6322.69	Fe I	2.59	−2.43	99.2	13
6481.87	Fe I	2.28	−2.98	84.3	13
6609.11	Fe I	2.56	−2.69	85.5	13
6739.52	Fe I	1.56	−4.82	30.8	13
6750.15	Fe I	2.42	−2.62	103.4	13
4656.98	Fe II	2.89	−3.55	27.8	14
4670.18	Fe II	2.58	−3.90	22.0	14
4993.36	Fe II	2.80	−3.49	36.2	14
5197.58	Fe II	3.23	−2.23	70.0	14
5425.26	Fe II	3.20	−3.37	31.5	14
6149.26	Fe II	3.89	−2.72	23.4	14
6247.56	Fe II	3.89	−2.33	35.7	14
6456.38	Fe II	3.90	−2.08	48.8	14
5342.71	Co I (Z= 27; $\log \epsilon_\odot = 4.91$)	4.02	0.54	40.2	7
5352.05	Co I	3.58	0.06	39.0	7
5647.23	Co I	2.28	−1.56	29.6	7
5578.73	Ni I (Z= 28; $\log \epsilon_\odot = 6.30$)	1.68	−2.79	72.1	3
5748.35	Ni I	1.68	−3.26	51.7	2
6007.31	Ni I	1.68	−3.34	42.2	2
6111.07	Ni I	4.09	−0.87	46.2	12

Table 1—Continued

λ (Å)	Species	χ_l	$\log gf$	EW$_\lambda$ (mÅ)	References
6128.96	Ni I	1.68	−3.43	45.0	12
6133.96	Ni I	4.09	−1.83	7.8	12
6176.81	Ni I	4.09	−0.35	81.2	12
6177.24	Ni I	1.83	−3.60	28.0	12
5105.00	Cu I (Z= 29; $\log \epsilon_\odot = 4.21$)	1.39	−1.52	Synth[a]	15
4722.15	Zn I (Z= 30; $\log \epsilon_\odot = 4.60$)	4.03	−0.34	Synth[a]	3
4810.53	Zn I	4.08	−0.14	Synth[a]	3
5087.43	Y II (Z= 39; $\log \epsilon_\odot = 2.12$)	1.08	−0.16	44.1	16
5402.78	Y II	1.84	−0.44	12.1	16
5853.67	Ba II (Z= 56; $\log \epsilon_\odot = 2.50$)	0.60	−1.01	66.6	7

[a]The abundance was determined from spectrum synthesis as no reliable EW measurement was available

References. — (1) Paulson et al. 2003; (2) Ramírez & Cohen 2002; (3) Kurucz & Bell 1995; (4) Garz 1973; (5) Smith & Raggett 1981; (6) Smith 1988; (7) Prochaska et al. 2000; (8) Blackwell 1982; (9) Blackwell 1986; (10) Blackwell 1983; (11) Savanov 1990; (12) Thorén & Feltzing 2000; (13) Lee & Carney 2002; (14) Biemont et al. 1991; (15) Simmerer et al. 2003; (16) Reddy et al. 2003

Note. — Spectral lines used in the elemental abundance analysis of the planet-host star TrES-1. Columns 1 through 6 report wavelength λ (in Å), species name, nominal solar abundance $\log \epsilon_\odot$ and Z number, lower excitation potential ξ_l (in eV), oscillator strengths $\log gf$, equivalent widths EW$_\lambda$ (in mÅ), and the reference number from which the $\log gf$ values were taken, respectively

Table 2. TrES-1: average abundance ratios

Species	Mean	σ	n
[Na/Fe]	−0.06	...	1
[Mg/Fe]	−0.04	0.05	3
[Al/Fe]	−0.07	0.03	2
[Si/Fe]	0.07	0.06	3
[Ca/Fe]	−0.06	0.09	4
[Sc/Fe]	−0.08	0.03	3
[Ti/Fe]	−0.03	0.05	15
[V/Fe]	0.00	0.03	4
[Cr/Fe]	0.10	...	1
[Mn/Fe]	0.09	...	1
[Fe/H]	0.00	0.09	36
[Co/Fe]	−0.05	0.04	3
[Ni/Fe]	0.07	0.05	8
[Cu/Fe]	−0.05	...	1
[Zn/Fe]	−0.13	0.04	2
[Y/Fe]	0.01	0.10	2
[Ba/Fe]	−0.05	...	1

Table 3. TrES-1: sensitivities to atmospheric parameters

Species	$\Delta T_{\rm eff} = +75$ K	$\Delta \log g = +0.2$ dex	$\Delta \xi_t = +0.10$ km s^{-1}
[Na/Fe]	0.05	−0.06	0.01
[Mg/Fe]	0.02	−0.04	0.02
[Al/Fe]	0.05	−0.06	0.01
[Si/Fe]	−0.01	−0.01	0.01
[Ca/Fe]	0.07	−0.08	0.01
[Sc/Fe]	-0.01	0.05	0.00
[Ti I/Fe]	0.10	−0.04	0.00
[Ti II/Fe]	0.01	0.03	0.00
[V/Fe]	0.10	−0.04	0.01
[Cr/Fe]	0.07	−0.05	0.02
[Mn/Fe]	0.07	−0.05	−0.01
[Co/Fe]	0.02	−0.01	0.01
[Ni/Fe]	0.04	−0.02	0.01
[Cu/Fe]	0.05	−0.05	−0.03
[Zn/Fe]	−0.01	−0.02	−0.01
[Y/Fe]	0.01	0.04	0.00
[Ba/Fe]	0.04	0.00	−0.04

Table 4. Kinematic data of stars with planets and TrES-1

Name	π (mas)	HRV km s^{-1}	μ_α mas yr^{-1}	μ_δ mas yr^{-1}	α (J2000) h:m:s	δ (J2000) d:m:s	U km s^{-1}	V km s^{-1}	W km s^{-1}	$P^{\rm thin}$ (M04)	$P^{\rm thick}$ (M04)	TD/D (B03)	$P_1^{\rm thin}$ (V04)	$P_1^{\rm thick}$ (V04)	$P_2^{\rm thin}$ (V04)	$P_2^{\rm thick}$ (V04)	X (S93)	[α/Fe]
TrES-1	6.66	−20.520	−42.00	−22.00	19 04 09.80	+36 37 57.5	−24.5	−21.4	23.1	0.92	0.08	0.02	0.70	0.30	1.00	0.00	−32.37	−0.00
HD142	39.00	2.600	575.21	−39.92	00 06 19.18	−49 04 30.7	49.2	−24.8	−5.8	0.92	0.08	0.02	0.70	0.30	1.00	0.00	−34.50	−0.01
HD1237	56.76	−5.808	433.88	−57.91	00 16 12.68	−79 51 04.3	24.1	−4.3	9.3	0.97	0.03	0.01	0.80	0.20	1.00	0.00	−36.76	−0.04
HD2039	11.13	8.400	78.53	15.23	00 24 20.28	−56 39 00.2	19.6	−2.6	−6.9	0.97	0.03	0.01	0.90	0.10	1.00	0.00	−40.72	−0.01
HD2638	18.62	9.550	−107.08	−224.06	00 29 59.87	−05 45 50.4	−59.7	−15.7	−20.3	0.90	0.10	0.03	0.60	0.30	1.00	0.00	−36.05	···
HD3651	90.03	−34.200	−461.09	−370.90	00 39 21.81	+21 15 01.7	−49.5	−8.3	16.2	0.94	0.06	0.02	0.80	0.20	1.00	0.00	−36.25	···
HD4203	12.85	−14.140	125.25	−123.99	00 44 41.20	+20 26 56.1	7.5	−47.2	−18.4	0.74	0.26	0.05	0.30	0.60	0.90	0.10	−36.47	0.01
HD4208	30.58	55.400	313.51	150.00	00 44 26.65	−26 30 56.4	43.5	7.1	−49.4	0.72	0.28	0.43	0.40	0.60	0.90	0.10	−31.52	0.06
HD6434	24.80	22.962	−168.97	−527.70	01 04 40.15	−39 29 17.6	−94.0	−55.0	4.4	0.23	0.77	0.83	0.10	0.80	0.70	0.30	−18.26	0.22
HD8574	22.65	18.864	252.59	−158.59	01 25 15.52	+28 34 00.1	35.1	−24.7	−23.8	0.90	0.10	0.03	0.60	0.40	1.00	0.00	−33.01	−0.04
HD9826	74.25	−27.700	−172.57	−381.03	01 36 47.84	+41 24 19.7	−37.1	−9.8	−7.5	0.96	0.04	0.01	0.80	0.20	1.00	0.00	−36.24	0.04
HD10647	57.63	12.900	166.97	−106.71	01 42 29.32	−53 44 27.0	−5.8	−7.9	2.1	0.97	0.03	0.00	0.90	0.10	1.00	0.00	−33.50	···
HD10697	30.71	−44.800	−45.05	−105.39	01 44 55.82	+20 04 59.3	−44.9	−15.6	23.1	0.92	0.08	0.02	0.70	0.30	1.00	0.00	−35.69	−0.01
HD12661	26.91	−52.200	−107.81	−175.26	02 04 34.29	+25 24 51.5	−63.8	−20.0	7.4	0.91	0.09	0.02	0.70	0.30	1.00	0.00	−39.23	−0.02
HD13445	91.63	56.570	2092.59	654.49	02 10 25.93	−50 49 25.4	88.6	−63.2	−22.6	0.08	0.92	3.00	0.00	0.90	0.40	0.60	−22.44	0.12
HD16141	27.85	−51.500	−156.89	−437.07	02 35 19.93	−03 33 38.2	−93.7	−29.4	9.0	0.70	0.30	0.15	0.40	0.60	0.90	0.10	−34.08	−0.03
HD17051	58.00	15.500	333.72	219.21	02 42 33.47	−50 48 01.1	22.2	−4.4	−0.6	0.97	0.03	0.01	0.90	0.10	1.00	0.00	−39.37	−0.05
HD19994	44.69	19.331	193.43	−69.23	03 12 46.44	−01 11 46.0	11.5	−7.4	0.1	0.97	0.03	0.00	0.90	0.10	1.00	0.00	−38.61	−0.02
HD20367	36.86	5.300	−103.09	−56.65	03 17 40.05	+31 07 37.4	−11.8	18.0	−7.5	0.96	0.04	0.01	0.90	0.10	1.00	0.00	−40.59	−0.08
HD22049	310.74	16.300	−976.36	17.98	03 32 55.84	−09 27 29.7	−5.4	19.0	−13.6	0.96	0.04	0.01	0.90	0.10	1.00	0.00	−35.12	0.03
HD23079	28.90	0.500	−193.62	−91.92	03 39 43.10	−52 54 57.0	−36.8	26.8	−8.5	0.94	0.06	0.02	0.90	0.10	1.00	0.00	−36.49	0.02
HD23596	19.24	−10.200	53.56	21.06	03 48 00.37	+40 31 50.3	−13.1	2.4	21.0	0.96	0.04	0.01	0.80	0.20	1.00	0.00	−41.20	−0.02
HD27442	54.84	29.300	−47.99	−167.81	04 16 29.03	−59 18 07.8	−24.1	−10.1	−12.1	0.96	0.04	0.01	0.80	0.20	1.00	0.00	−41.06	−0.03
HD27894	23.60	82.900	182.25	272.33	04 20 47.05	−59 24 39.0	54.3	−61.3	−35.6	0.13	0.87	1.80	0.00	0.90	0.50	0.50	−32.78	···
HD28185	25.28	50.246	80.85	−60.29	04 26 26.32	−10 33 02.9	24.6	−22.7	−16.2	0.93	0.07	0.01	0.70	0.30	1.00	0.00	−36.26	−0.04
HD33636	34.85	5.300	180.83	−137.32	05 11 46.45	+04 24 12.7	−8.8	−18.0	16.0	0.95	0.05	0.01	0.80	0.20	1.00	0.00	−31.48	0.01
HD37124	30.08	−19.000	−79.75	−419.96	05 37 02.49	+20 43 50.8	−37.6	−34.7	−36.4	0.70	0.30	0.15	0.30	0.70	0.90	0.10	−23.50	0.17
HD37605	23.32	−22.050	54.70	−245.76	05 40 01.73	+06 03 38.1	−48.4	−26.0	−2.7	0.92	0.08	0.02	0.70	0.30	1.00	0.00	−37.51	···
HD38529	23.57	30.000	−80.05	−141.79	05 46 34.91	+01 10 05.5	4.3	−13.1	−27.0	0.94	0.06	0.02	0.70	0.30	1.00	0.00	−40.86	−0.00
HD39091	54.92	9.400	311.88	1050.20	05 37 09.89	−80 28 08.8	74.1	−33.9	6.5	0.78	0.22	0.06	0.40	0.50	0.90	0.10	−32.58	−0.01
HD40979	30.00	32.800	95.05	−152.23	06 04 29.94	+44 15 37.6	27.7	−9.3	15.3	0.96	0.04	0.01	0.80	0.20	1.00	0.00	−37.80	···
HD41004A	23.24	42.200	−42.27	65.16	05 59 49.65	−48 14 22.9	13.7	−17.5	−18.3	0.95	0.05	0.01	0.70	0.30	1.00	0.00	−35.81	···
HD46375	29.93	4.000	114.24	−96.79	06 33 12.62	+05 27 46.5	−14.8	−9.5	15.8	0.96	0.04	0.01	0.80	0.20	1.00	0.00	−37.59	0.05
HD47536	8.24	78.800	108.96	64.13	06 37 47.62	−32 20 23.0	46.8	−67.0	53.1	0.02	0.98	31.00	0.00	0.90	0.10	0.90	−16.34	···
HD49674	24.55	11.80	34.96	−122.85	06 51 30.52	+40 52 03.9	4.8	−11.5	8.3	0.97	0.03	0.01	0.80	0.20	1.00	0.00	−39.77	···
HD50554	32.23	−3.861	−37.29	−96.36	06 54 42.83	+24 14 44.0	−12.6	1.9	−4.4	0.97	0.03	0.01	0.90	0.10	1.00	0.00	−35.52	0.00
HD52265	35.63	53.600	−115.76	80.35	07 00 18.04	−05 22 01.8	43.1	−8.5	−2.2	0.96	0.04	0.01	0.80	0.20	1.00	0.00	−38.28	−0.04
HD59686	10.81	−40.200	42.65	−75.39	07 31 48.40	+17 05 09.8	−59.7	−8.4	−0.8	0.94	0.06	0.01	0.80	0.20	1.00	0.00	−39.23	···
HD63454	27.93	33.840	−20.65	−39.69	07 39 21.85	−78 16 44.3	−24.0	−13.0	−11.7	0.96	0.04	0.01	0.80	0.20	1.00	0.00	−35.46	···
HD65216	28.10	42.300	−122.12	145.90	07 53 41.32	−63 38 50.4	17.8	−29.1	−13.2	0.92	0.08	0.01	0.60	0.30	1.00	0.00	−29.08	···
HD68988	17.00	−69.700	128.33	31.73	08 18 22.17	+61 27 38.6	−84.1	−9.5	−2.9	0.88	0.12	0.04	0.70	0.30	1.00	0.00	−40.58	···
HD70642	34.77	48.100	−202.07	225.59	08 21 28.14	−39 42 19.5	41.2	−26.0	0.4	0.93	0.07	0.01	0.70	0.30	1.00	0.00	−35.09	···
HD72659	19.47	−18.400	−113.75	−98.30	08 34 03.19	−01 34 05.6	−16.4	10.0	−33.2	0.92	0.08	0.04	0.80	0.20	1.00	0.00	−36.94	···
HD73256	27.38	29.500	−180.58	65.71	08 36 23.02	−30 02 15.5	27.2	−8.9	−7.9	0.96	0.04	0.01	0.80	0.20	1.00	0.00	−38.79	···
HD73526	10.57	26.100	−60.31	161.70	08 37 16.48	−41 19 08.8	68.3	−1.8	29.1	0.86	0.14	0.08	0.60	0.40	1.00	0.00	−39.90	···
HD74156	15.49	3.813	24.96	−200.48	08 42 55.12	+04 34 41.2	−37.6	−39.8	−11.1	0.83	0.17	0.03	0.50	0.50	0.90	0.10	−32.94	−0.02
HD75289	34.55	9.258	−20.50	−227.68	08 47 40.39	−41 44 12.4	−30.0	−0.6	−14.6	0.96	0.04	0.01	0.80	0.20	1.00	0.00	−40.24	−0.04
HD75732	79.80	27.800	−485.46	−234.40	08 52 35.81	+28 19 50.9	28.4	−6.2	−0.7	0.97	0.03	0.01	0.80	0.20	1.00	0.00	−40.44	0.01
HD76700	16.75	36.700	−283.05	121.22	08 53 55.52	−66 48 03.6	59.9	−29.3	−42.7	0.57	0.43	0.46	0.20	0.80	0.80	0.20	−38.96	···
HD80606	17.13	3.768	46.98	6.92	09 22 37.57	+50 36 13.4	−15.7	14.8	18.5	0.96	0.04	0.01	0.90	0.10	1.00	0.00	−42.98	0.00
HD82943	36.42	8.060	2.38	−174.05	09 34 50.74	−12 07 46.4	−19.2	−7.8	−1.8	0.97	0.03	0.01	0.80	0.20	1.00	0.00	−39.68	−0.06
HD83443	22.97	28.917	22.35	−120.76	09 37 11.83	−43 16 19.9	−28.9	−18.6	−4.8	0.95	0.05	0.01	0.80	0.20	1.00	0.00	−39.22	0.01
HD88133	13.43	−3.53	−12.87	−263.91	10 10 07.68	+18 11 12.7	−39.6	−72.2	−19.0	0.11	0.89	1.10	0.10	0.90	0.50	0.50	−31.93	···

Table 4—Continued

Name	π (mas)	HRV km s^{-1}	μ_α mas yr^{-1}	μ_δ mas yr^{-1}	α (J2000) h:m:s	δ (J2000) d:m:s	U km s^{-1}	V km s^{-1}	W km s^{-1}	$P^{\rm thin}$ (M04)	$P^{\rm thick}$ (M04)	TD/D (B03)	$P_1^{\rm thin}$ (V04)	$P_1^{\rm thick}$ (V04)	$P_2^{\rm thin}$ (V04)	$P_2^{\rm thick}$ (V04)	X (S93)	[α/Fe]
HD89744	25.65	6.500	−120.17	−138.60	10 22 10.56	+41 13 46.3	8.6	−17.4	3.5	0.96	0.04	0.01	0.80	0.20	1.00	0.00	−36.95	···
HD92788	30.94	−4.000	−12.63	−222.75	10 42 48.53	−02 11 01.5	−25.0	−10.6	−13.3	0.96	0.04	0.01	0.80	0.20	1.00	0.00	−39.70	−0.02
HD93083	34.60	41.70	−92.84	−151.12	10 44 20.91	−33 34 37.3	−12.3	−35.6	0.2	0.91	0.09	0.01	0.60	0.40	1.00	0.00	−33.29	···
HD95128	71.04	12.000	−315.92	55.15	10 59 27.97	+40 25 48.9	15.3	9.5	8.3	0.97	0.03	0.01	0.90	0.10	1.00	0.00	−37.44	−0.01
HD99492	55.59	1.700	−730.15	191.17	11 26 46.28	+03 00 22.8	53.2	0.7	−4.8	0.95	0.05	0.01	0.80	0.20	1.00	0.00	−40.05	···
HD101930	32.79	18.360	15.00	347.49	11 43 30.11	−58 00 24.8	−5.1	−6.3	57.1	0.63	0.37	0.80	0.20	0.70	0.80	0.20	−37.44	···
HD102117	23.81	48.90	−63.05	−69.87	11 44 50.46	−58 42 13.4	−21.6	−36.8	−7.0	0.89	0.11	0.02	0.60	0.40	1.00	0.00	−36.31	···
HD104985	9.80	−19.800	147.22	−92.36	12 05 15.12	+76 54 20.6	−88.2	3.6	40.3	0.63	0.37	0.65	0.40	0.60	0.90	0.10	−30.32	···
HD106252	26.71	15.481	23.77	−279.41	12 13 29.51	+10 02 29.9	−37.5	−31.6	7.5	0.90	0.10	0.02	0.60	0.40	1.00	0.00	−30.82	−0.03
HD108147	25.93	−5.065	−181.60	−60.80	12 25 46.27	−64 01 19.5	21.3	0.6	−7.2	0.97	0.03	0.01	0.90	0.10	1.00	0.00	−38.90	−0.05
HD108874	14.59	−30.700	129.16	−89.40	12 30 26.88	+22 52 47.4	−60.8	11.6	−22.2	0.91	0.09	0.04	0.80	0.20	1.00	0.00	−40.89	−0.04
HD111232	34.63	102.200	27.82	112.81	12 48 51.75	−68 25 30.5	−67.8	−72.8	12.5	0.07	0.93	2.10	0.00	0.90	0.40	0.60	−18.95	···
HD114386	35.66	33.370	−138.23	−325.10	13 10 39.82	−35 03 17.2	−21.1	−40.1	−14.2	0.84	0.16	0.03	0.50	0.50	0.90	0.10	−28.41	0.07
HD114729	28.57	64.700	−202.11	−308.49	13 12 44.26	−31 52 24.1	−28.3	−74.5	−0.8	0.12	0.88	0.65	0.10	0.90	0.50	0.50	−20.79	0.07
HD114762	24.65	49.300	−582.68	−1.98	13 12 19.74	+17 31 01.6	73.9	−57.3	64.4	0.01	0.99	220.00	0.00	0.90	0.10	0.90	−14.60	0.19
HD114783	48.95	−12.800	−138.13	9.62	13 12 43.79	−02 15 54.1	6.7	9.5	−2.5	0.97	0.03	0.01	0.90	0.10	1.00	0.00	−38.00	−0.01
HD117176	55.22	5.200	−234.81	−576.19	13 28 25.81	+13 46 43.6	−22.1	−39.9	3.3	0.87	0.13	0.02	0.50	0.50	0.90	0.10	−28.81	0.02
HD117207	30.29	−17.900	−204.99	−71.73	13 29 21.11	−35 34 15.6	24.9	−0.1	−6.2	0.97	0.03	0.01	0.90	0.10	1.00	0.00	−39.36	···
HD117618	26.30	0.900	25.04	−124.63	13 32 25.56	−47 16 16.9	−13.9	7.2	−14.8	0.97	0.03	0.01	0.90	0.10	1.00	0.00	−37.15	···
HD120136	64.12	−15.800	−480.34	54.18	13 47 15.74	+17 27 24.9	24.5	−6.7	0.1	0.97	0.03	0.01	0.80	0.20	1.00	0.00	−38.51	···
HD121504	22.54	19.548	−250.55	−84.02	13 57 17.24	−56 02 24.2	18.8	−39.8	5.2	0.87	0.13	0.02	0.50	0.50	0.90	0.10	−32.93	−0.05
HD128311	60.35	−9.600	205.46	−249.68	14 36 00.56	+09 44 47.5	−25.8	7.5	−13.7	0.96	0.04	0.01	0.90	0.10	1.00	0.00	−36.62	−0.01
HD130322	33.60	−12.504	−129.60	−140.79	14 47 32.73	−00 16 53.3	0.3	−14.0	−3.8	0.97	0.03	0.01	0.80	0.20	1.00	0.00	−33.83	−0.00
HD134987	38.98	5.200	−399.01	−75.10	15 13 28.67	−25 18 33.6	11.5	−28.0	27.8	0.88	0.12	0.03	0.50	0.50	0.90	0.10	−37.07	−0.00
HD136118	19.13	−3.600	−124.05	23.50	15 18 55.47	−01 35 32.6	12.3	−4.0	23.6	0.95	0.05	0.01	0.80	0.20	1.00	0.00	−33.81	0.03
HD137759	31.92	−10.700	−8.27	17.30	15 24 55.77	+58 57 57.8	−6.6	5.0	−1.2	0.97	0.03	0.01	0.90	0.10	1.00	0.00	−38.06	−0.03
HD141937	29.89	−2.994	97.12	24.00	15 52 17.55	−18 26 09.8	−11.9	25.2	−1.6	0.96	0.04	0.01	0.90	0.10	1.00	0.00	−40.22	0.04
HD142022	27.88	−10.500	−337.60	−31.10	16 10 15.02	−84 13 53.8	21.1	−18.5	46.8	0.75	0.25	0.21	0.30	0.70	0.90	0.10	−36.24	···
HD142415	28.93	−12.000	−113.96	−102.35	15 57 40.79	−60 12 00.9	15.4	−1.3	7.4	0.97	0.03	0.01	0.90	0.10	1.00	0.00	−38.84	···
HD143761	57.38	18.000	−196.88	−773.00	16 01 02.66	+33 18 12.6	−63.1	−23.9	28.0	0.81	0.19	0.08	0.50	0.50	0.90	0.10	−28.06	0.09
HD145675	55.11	−13.842	132.52	−298.38	16 10 24.31	+43 49 03.5	−32.8	−0.3	−9.0	0.96	0.04	0.01	0.90	0.10	1.00	0.00	−43.08	−0.06
HD147513	77.69	10.100	72.64	3.41	16 24 01.29	−39 11 34.7	−19.8	11.7	5.2	0.97	0.03	0.01	0.90	0.10	1.00	0.00	−37.73	−0.02
HD150706	36.73	−14.000	95.83	−87.97	16 31 17.59	+79 47 23.2	−27.2	9.8	−4.7	0.97	0.03	0.01	0.90	0.10	1.00	0.00	−36.17	−0.04
HD154857	14.59	27.900	87.19	−55.37	17 11 15.72	−56 40 50.9	−29.0	3.6	−30.8	0.93	0.07	0.03	0.70	0.20	1.00	0.00	−31.25	···
HD160691	65.46	−9.000	−15.06	−191.17	17 44 08.70	−51 50 02.6	4.6	3.5	3.0	0.97	0.03	0.00	0.90	0.10	1.00	0.00	−41.53	−0.03
HD162020	31.99	−27.600	20.99	−25.20	17 50 38.36	−40 19 06.1	18.8	14.8	5.6	0.97	0.03	0.01	0.90	0.10	1.00	0.00	−36.25	−0.02
HD168443	26.40	−49.000	−92.15	−224.16	18 20 03.93	−09 35 44.6	21.1	−45.8	0.5	0.80	0.20	0.03	0.40	0.60	0.90	0.10	−30.30	0.04
HD168746	23.19	−25.645	−22.13	−69.23	18 21 49.78	−11 55 21.7	10.4	−10.1	3.8	0.97	0.03	0.01	0.80	0.20	1.00	0.00	−32.28	0.12
HD169830	27.53	−17.215	−0.84	−15.16	18 27 49.48	−29 49 00.7	7.9	8.4	8.5	0.97	0.03	0.01	0.90	0.10	1.00	0.00	−40.11	−0.07
HD177830	16.94	−72.300	−40.68	−51.84	19 05 20.77	+25 55 14.4	14.2	−58.5	−0.0	0.55	0.45	0.09	0.20	0.80	0.80	0.20	−33.70	0.03
HD178911	20.42	−40.432	47.12	194.51	19 09 04.38	+34 36 01.6	49.4	−7.3	7.8	0.95	0.05	0.01	0.80	0.20	1.00	0.00	−39.18	···
HD179949	36.97	−25.500	114.78	−101.81	19 15 33.23	−24 10 45.7	18.3	−0.9	−4.0	0.97	0.03	0.01	0.90	0.10	1.00	0.00	−39.07	−0.04
HD183263	18.93	−50.700	−17.78	−33.14	19 28 24.57	+08 21 29.0	20.3	−30.2	10.8	0.92	0.08	0.01	0.60	0.30	1.00	0.00	−37.54	···
HD186427	46.70	−27.500	−135.15	−163.53	19 41 51.97	+50 31 03.1	−26.6	−18.1	5.3	0.95	0.05	0.01	0.80	0.20	1.00	0.00	−34.24	−0.02
HD187123	20.87	−17.500	143.13	−123.23	19 46 58.11	+34 25 10.3	−11.6	−3.9	−36.4	0.91	0.09	0.04	0.70	0.30	1.00	0.00	−37.01	−0.05
HD188015	19.00	2.600	53.89	−91.03	19 52 04.54	+28 06 01.4	−21.6	9.1	−16.1	0.96	0.04	0.01	0.90	0.10	1.00	0.00	−41.87	···
HD190228	16.10	−50.218	104.91	−69.85	20 03 00.77	+28 18 24.7	10.8	−35.1	−28.8	0.82	0.18	0.05	0.40	0.60	0.90	0.10	−25.70	0.05
HD190360	62.92	−45.300	683.35	−524.10	20 03 37.41	+29 53 48.5	3.1	−32.8	−57.0	0.37	0.63	1.70	0.10	0.90	0.60	0.40	−35.34	0.00
HD192263	50.27	−10.817	−63.37	262.26	20 13 59.85	−00 52 00.8	7.5	22.1	26.6	0.93	0.07	0.03	0.80	0.20	1.00	0.00	−37.57	0.01
HD195019	26.77	−93.100	349.49	−56.85	20 28 18.64	+18 46 10.2	63.5	−65.1	−30.2	0.10	0.90	2.20	0.00	0.90	0.40	0.60	−28.18	−0.00
HD196050	21.31	60.900	−190.97	−64.27	20 37 51.71	−60 38 04.1	−74.5	−25.6	6.4	0.85	0.15	0.05	0.60	0.40	1.00	0.00	−35.89	−0.00
HD202206	21.58	14.720	−38.23	−119.77	21 14 57.77	−20 47 21.2	−31.6	−7.2	−2.8	0.96	0.04	0.01	0.80	0.20	1.00	0.00	−40.69	−0.06
HD208487	22.73	5.300	101.45	−117.99	21 57 19.85	−37 45 49.0	0.8	−14.8	−9.2	0.96	0.04	0.01	0.80	0.20	1.00	0.00	−34.29	···
HD209458	21.24	−14.765	28.90	−18.37	22 03 10.77	+18 53 03.5	−3.3	−3.6	7.5	0.97	0.03	0.01	0.90	0.10	1.00	0.00	−34.99	−0.02

Table 4—Continued

Name	π (mas)	HRV km s^{-1}	μ_α mas yr^{-1}	μ_δ mas yr^{-1}	α (J2000) h:m:s	δ (J2000) d:m:s	U km s^{-1}	V km s^{-1}	W km s^{-1}	$P^{\rm thin}$ (M04)	$P^{\rm thick}$ (M04)	TD/D (B03)	$P_1^{\rm thin}$ (V04)	$P_1^{\rm thick}$ (V04)	$P_2^{\rm thin}$ (V04)	$P_2^{\rm thick}$ (V04)	X (S93)	[α/Fe]
HD210277	46.97	−21.100	85.48	−449.83	22 09 29.87	−07 32 55.2	−12.9	−38.2	0.9	0.89	0.11	0.02	0.60	0.40	1.00	0.00	−33.70	0.04
HD213240	24.54	−0.458	−135.16	−194.06	22 31 00.37	−49 25 59.8	−34.2	−18.0	30.3	0.89	0.11	0.04	0.60	0.40	1.00	0.00	−35.93	−0.03
HD216435	30.04	−1.100	216.70	−81.49	22 53 37.93	−48 35 53.8	18.4	−9.7	−3.4	0.97	0.03	0.01	0.80	0.20	1.00	0.00	−38.32	−0.04
HD216437	37.71	−3.000	−43.19	73.20	22 54 39.48	−70 04 25.4	−12.2	22.5	6.1	0.96	0.04	0.01	0.90	0.10	1.00	0.00	−42.67	−0.04
HD216770	26.39	30.700	228.60	−178.18	22 55 53.71	−26 39 31.5	3.1	−23.7	−40.1	0.82	0.18	0.09	0.40	0.60	0.90	0.10	−36.87	···
HD217014	65.10	−33.600	208.07	60.96	22 57 27.98	+20 46 07.8	6.2	−17.9	22.8	0.94	0.06	0.01	0.70	0.30	1.00	0.00	−36.51	−0.00
HD217107	50.71	−14.000	−6.05	−16.03	22 58 15.54	−02 23 43.4	−7.4	3.1	17.8	0.96	0.04	0.01	0.90	0.10	1.00	0.00	−42.40	−0.04
HD219449	21.97	−26.400	368.56	−17.02	23 15 53.49	−09 05 15.9	63.2	−29.9	0.2	0.86	0.14	0.03	0.60	0.40	1.00	0.00	−32.15	···
HD222404	72.50	−42.400	−48.85	127.19	23 39 20.85	+77 37 56.2	−30.5	−25.4	4.3	0.94	0.06	0.01	0.70	0.30	1.00	0.00	−34.79	···
HD222582	23.84	12.067	−145.41	−111.10	23 41 51.53	−05 59 08.7	−45.6	11.4	−4.1	0.96	0.04	0.01	0.90	0.10	1.00	0.00	−37.50	−0.05
HD330075	19.92	61.280	−235.58	−94.14	15 49 37.69	−49 57 48.7	−31.9	−68.1	28.1	0.13	0.87	1.10	0.10	0.90	0.50	0.50	−27.79	···
BD-103166	10.00	26.400	−183.00	−4.80	10 58 28.78	+10 46 13.4	71.3	−27.4	−7.6	0.85	0.15	0.04	0.50	0.40	0.90	0.10	−38.08	···
GJ876	212.69	−1.902	960.31	−675.61	22 53 16.73	−14 15 49.3	3.5	−7.9	−4.5	0.97	0.03	0.00	0.80	0.10	1.00	0.00	...	···
GJ436	97.73	10.000	896.34	−813.70	11 42 11.09	+26 42 23.7	−61.5	−7.4	27.1	0.89	0.11	0.05	0.60	0.40	1.00	0.00	...	···

Note. — Spatial properties and population assignments for stars with planets and TrES-1. For each entry in the table, the 19 columns report star name, parallax (π), heliocentric radial-velocity (HRV), proper motion in right ascension and declination (μ_α and μ_δ), equatorial coordinates (α and δ), galactic velocity vector (U, V, and W), thin and thick disk membership probabilities $P^{\rm thin}$ and $P^{\rm thick}$ according to Mishenina et al. (2004) (M04), the thick-to-thin disk probability ratio values TD/D according to Bensby et al. (2003) (B03)), thin and thick disk membership probabilities according to Venn et al. (2004) (V04), assuming both uniform and Bensby's prior probability distributions ($P_1^{\rm thin}$, $P_1^{\rm thick}$ and $P_2^{\rm thin}$, $P_2^{\rm thick}$, respectively), the X stellar population criterion according to Schuster et al. (1993) (S93), and the abundance ratio [α/Fe] from Bodaghee et al. (2003) and Beirão et al. (2005). All values of positions, proper motions, and parallax are taken from *Hipparcos* (ESA 1997) and the SIMBAD database, except for TrES-1, for which RA, DEC, μ_α and μ_δ were taken from the USNO-B1.0 catalog (Monet et al. 2003), while the photometric parallax estimate was taken from Sozzetti et al. (2004). The values of heliocentric radial-velocity are taken from SIMBAD and from the corresponding planet discovery papers.

Table 5. Results of the K-S tests

Samples	$Pr(D)$ (All [Fe/H])	$Pr(D)$ ([Fe/H]$\leq$ 0.0)	$Pr(D)$ ([Fe/H]$>$ 0.0)
$[\alpha/\mathrm{Fe}]_{\mathrm{pl}}$ vs. $[\alpha/\mathrm{Fe}]_{\mathrm{cs}}$	5.34×10^{-10}	0.24	2.41×10^{-3}
$[\alpha/\mathrm{Fe}]_{\mathrm{pl}}$ vs. $[\alpha/\mathrm{Fe}]_{\mathrm{SG}}$	2.94×10^{-30}	2.26×10^{-3}	1.78×10^{-23}
$[\alpha/\mathrm{Fe}]_{\mathrm{cs}}$ vs. $[\alpha/\mathrm{Fe}]_{\mathrm{SG}}$	0.06	0.21	0.07

Note. — Results of the K-S test on different stellar samples: $[\alpha/\mathrm{Fe}]_{\mathrm{pl}}$ and $[\alpha/\mathrm{Fe}]_{\mathrm{cs}}$ are the distributions of $[\alpha/\mathrm{Fe}]$ abundances for the samples of planet hosts and comparison field stars from Bodaghee et al. (2003) and Beirão et al. (2005), while $[\alpha/\mathrm{Fe}]_{\mathrm{SG}}$ is the analogous distribution from the Soubiran & Girard (2005) sample. The significance level $Pr(D)$ is calculated when comparing the $[\alpha/\mathrm{Fe}]$ distributions in three cases: a) for all values of [Fe/H], b) for [Fe/H]$\leq$ 0.0, and c) for [Fe/H]$>$ 0.0.

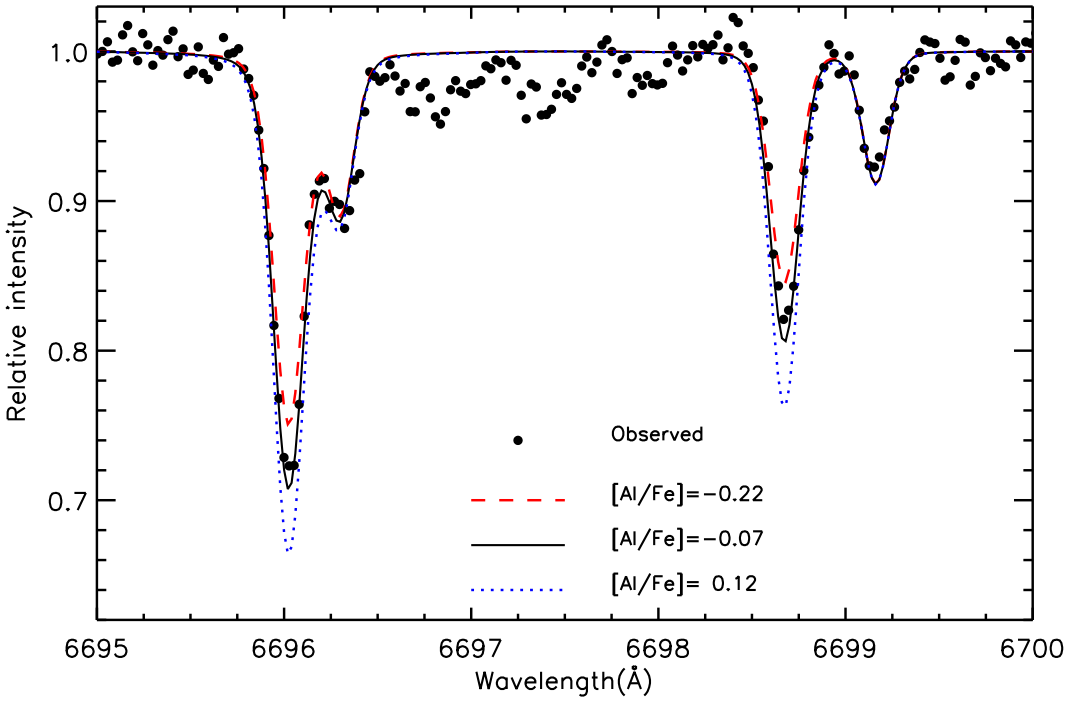
Relative intensity
1.0
0.9
0.8
0.7
Observed
[Al/Fe]=−0.22
[Al/Fe]=−0.07
[Al/Fe]= 0.12
6695
6696
6697
6698
6699
6700
Wavelength(Å)

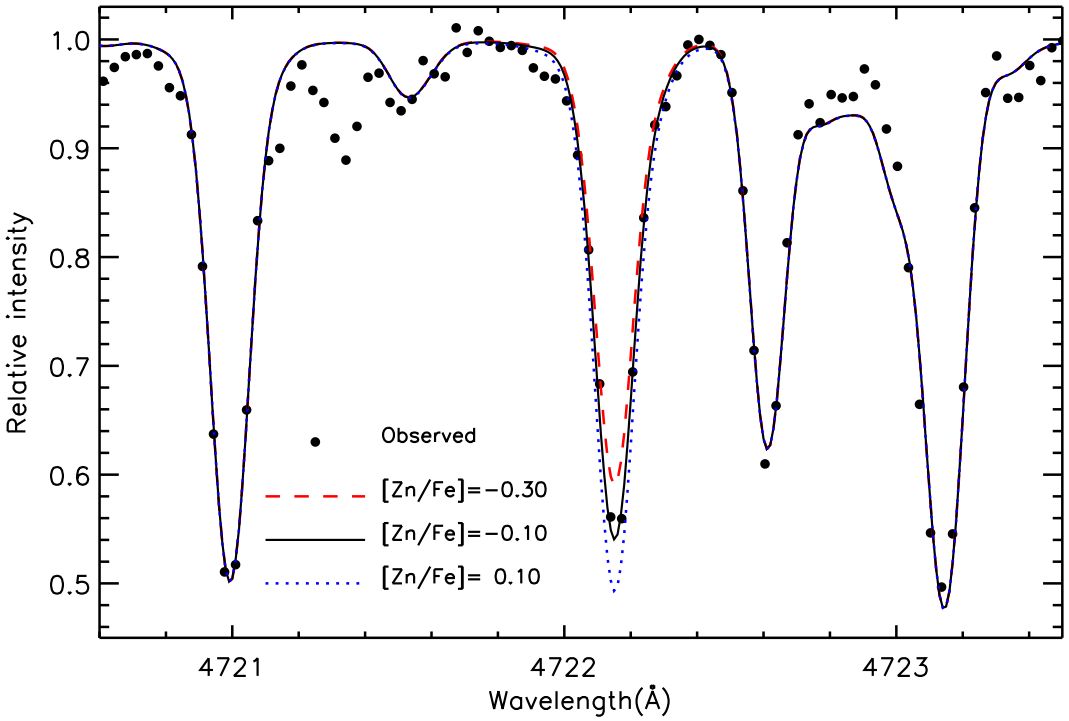
Relative intensity
1.0
0.9
0.8
0.7
0.6
0.5
Observed
[Zn/Fe]=−0.30
[Zn/Fe]=−0.10
[Zn/Fe]= 0.10
4721
4722
4723
Wavelength(Å)

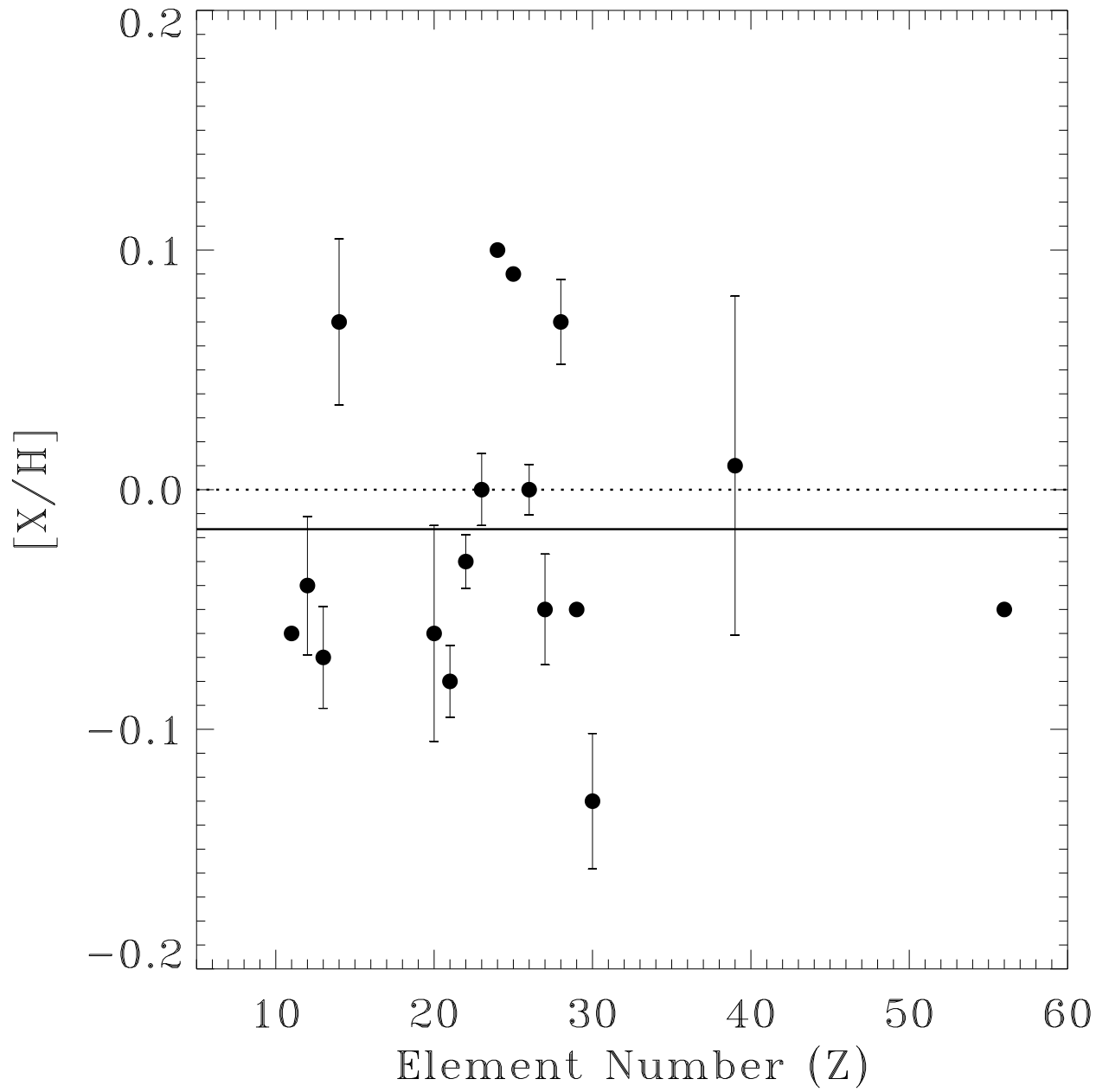
0.2
0.1
0.0
−0.1
−0.2
[X/H]
10
20
30
40
50
60
Element Number (Z)

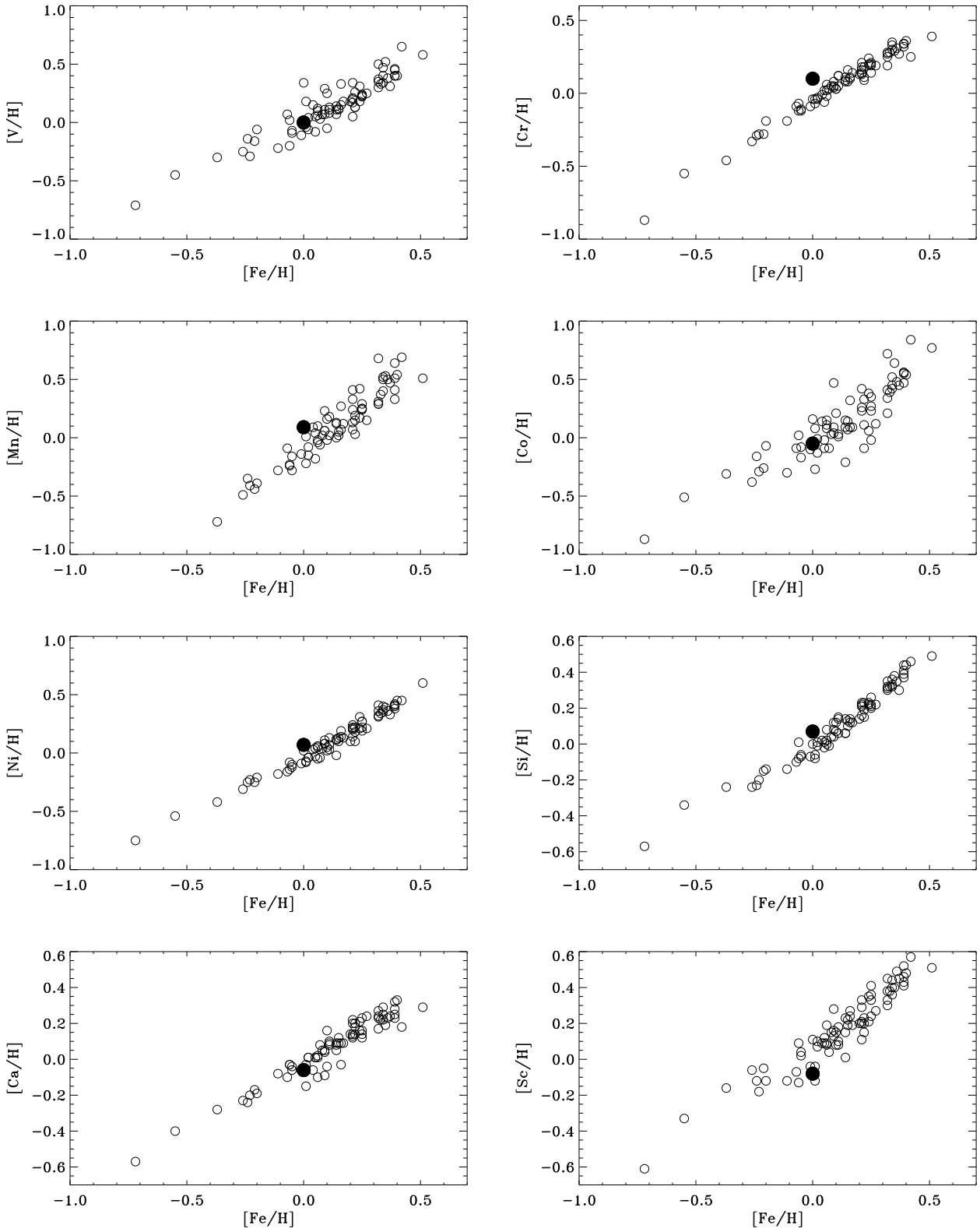
[V/H]
[Fe/H]
[Cr/H]
[Fe/H]
[Mn/H]
[Fe/H]
[Co/H]
[Fe/H]
[Ni/H]
[Fe/H]
[Si/H]
[Fe/H]
[Ca/H]
[Fe/H]
[Sc/H]
[Fe/H]

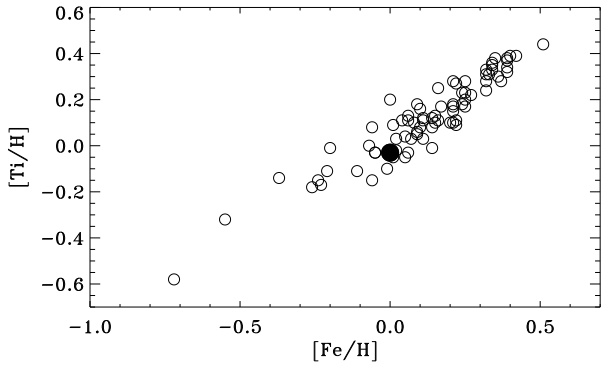
[Ti/H]
[Fe/H]

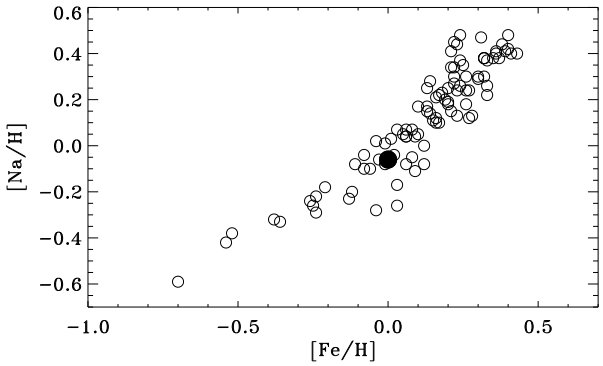
[Na/H]
[Fe/H]

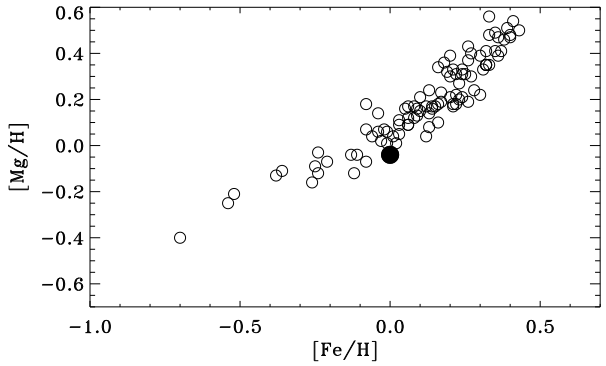
[Mg/H]
[Fe/H]

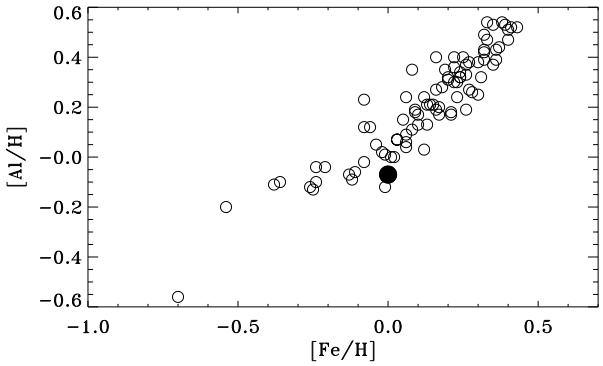
[Al/H]
[Fe/H]

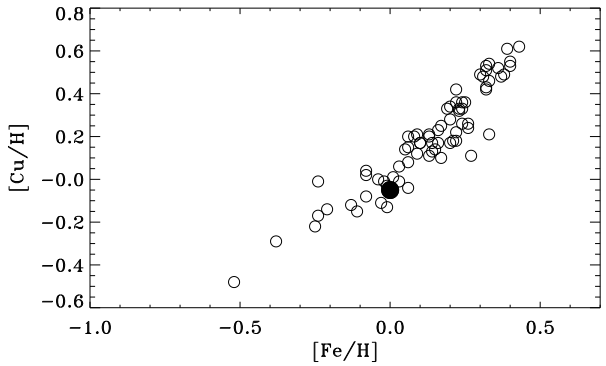
[Cu/H]
[Fe/H]

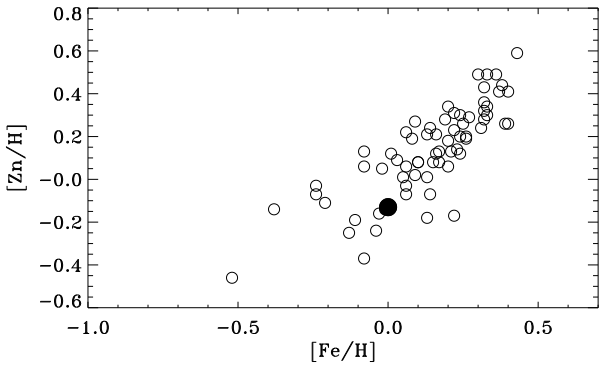
[Zn/H]
[Fe/H]

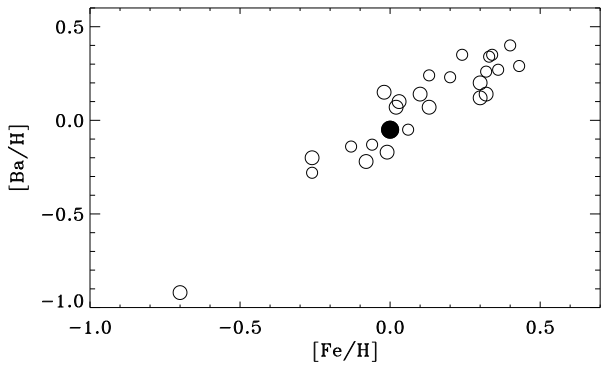
[Ba/H]
[Fe/H]

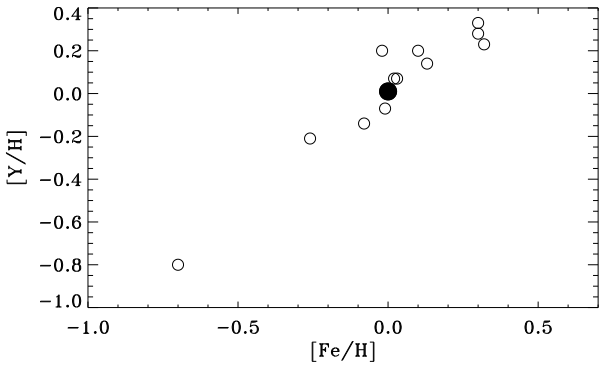
[Y/H]
[Fe/H]

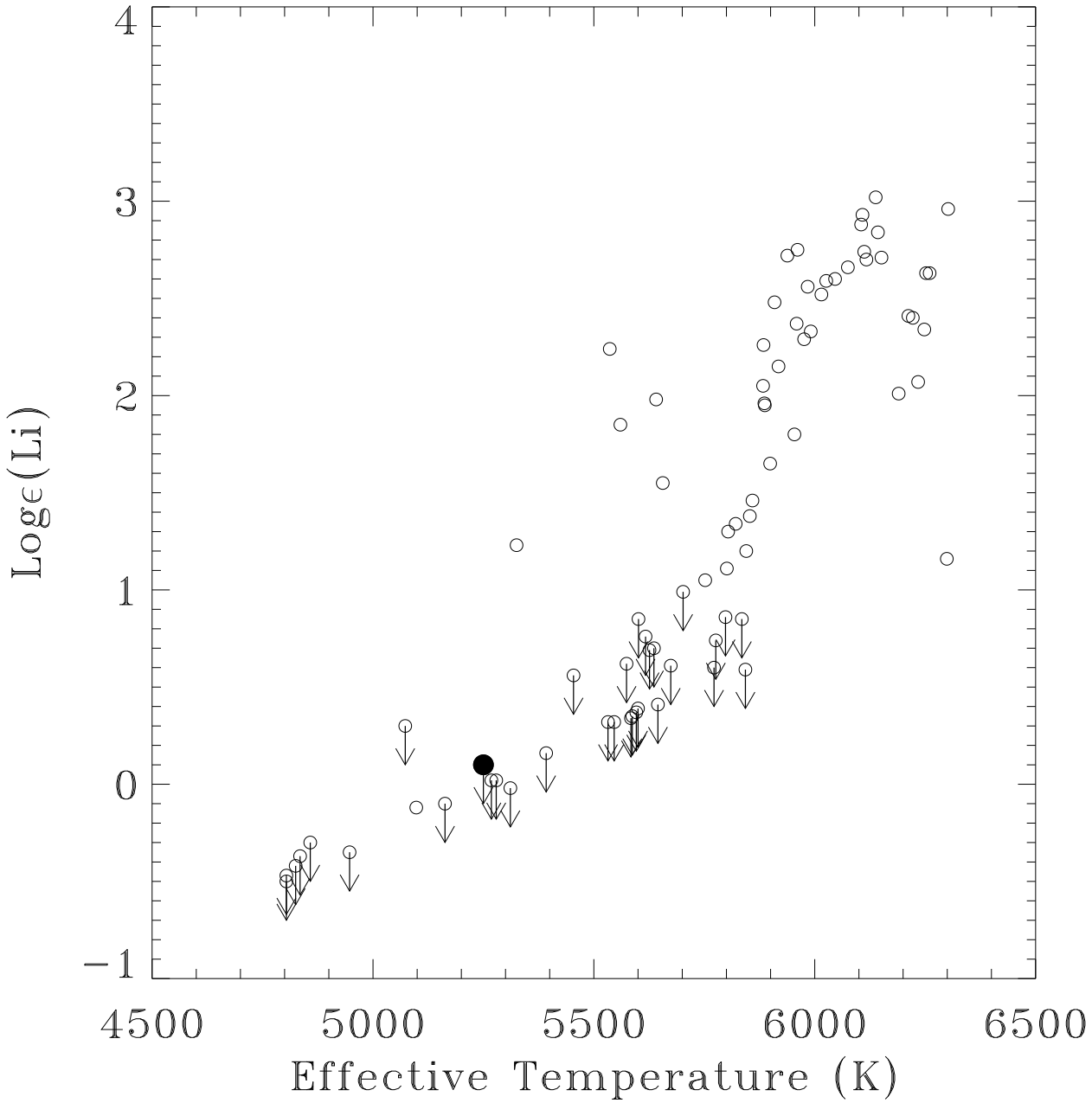
4
3
2
1
0
−1
Log∈(Li)
4500
5000
5500
6000
6500
Effective Temperature (K)

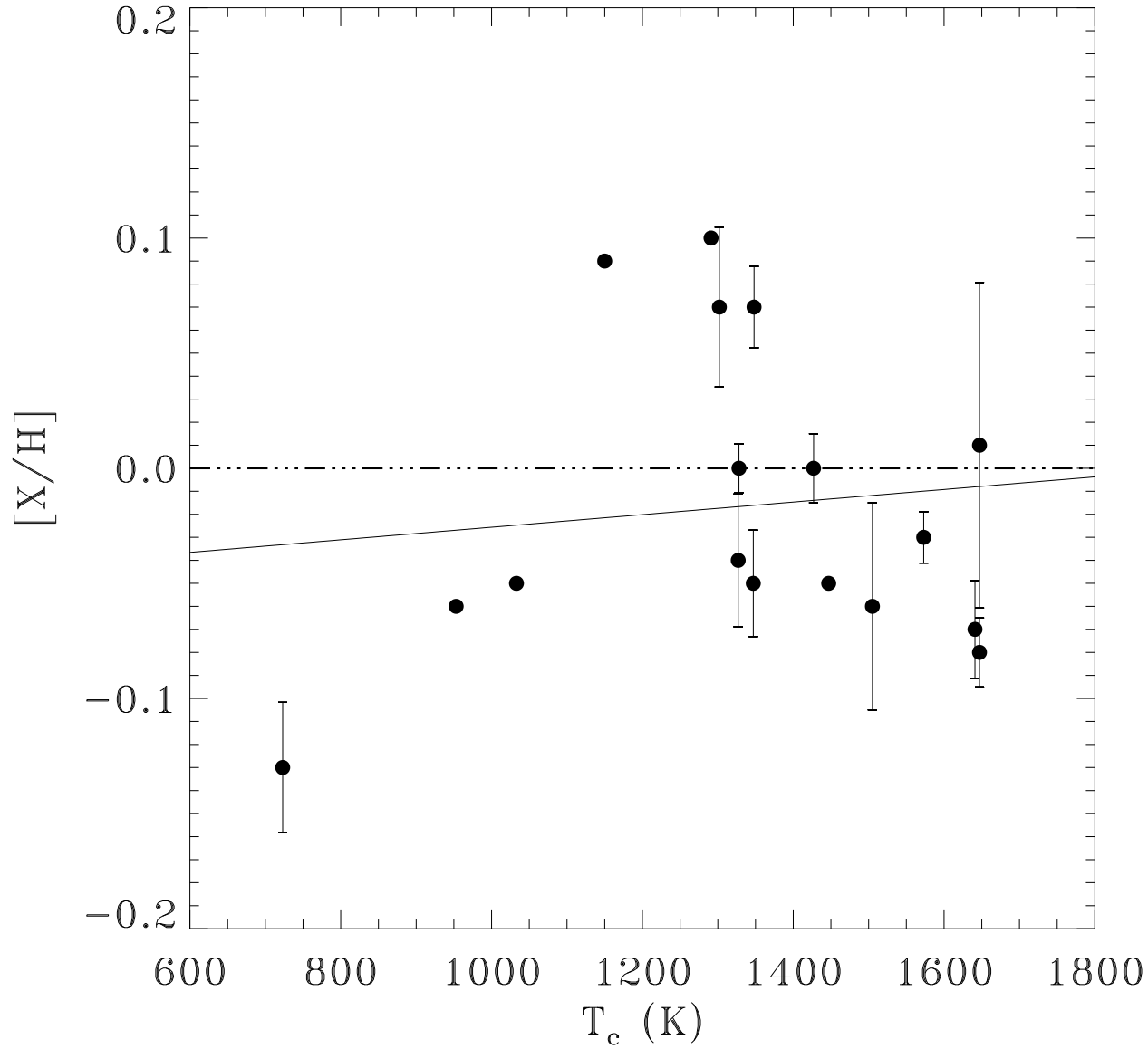
0.2
0.1
0.0
−0.1
−0.2
[X/H]
600
800
1000
1200
1400
1600
1800
T_c (K)

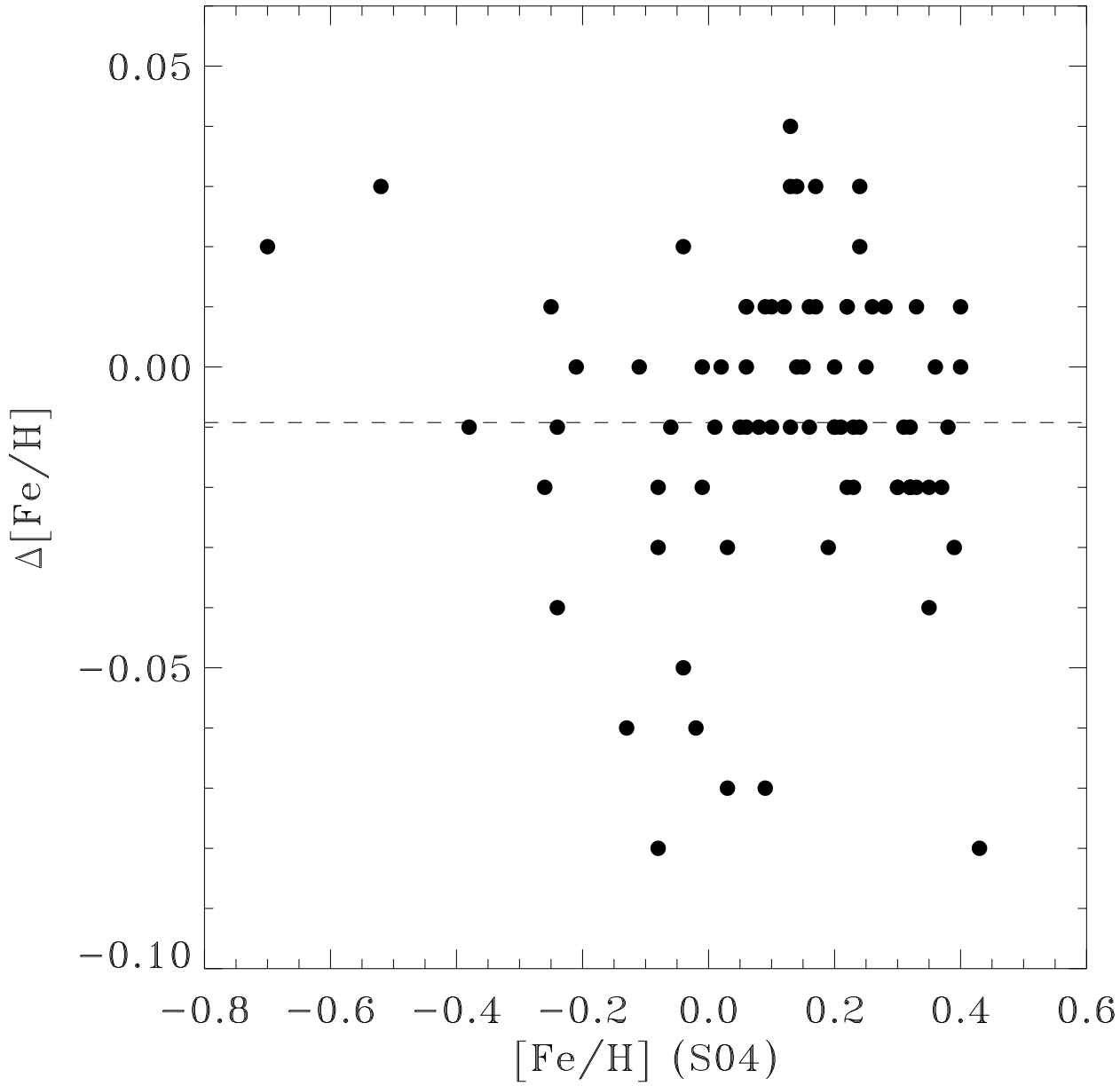
0.05
0.00
−0.05
−0.10
Δ[Fe/H]
−0.8
−0.6
−0.4
−0.2
0.0
0.2
0.4
0.6
[Fe/H] (S04)

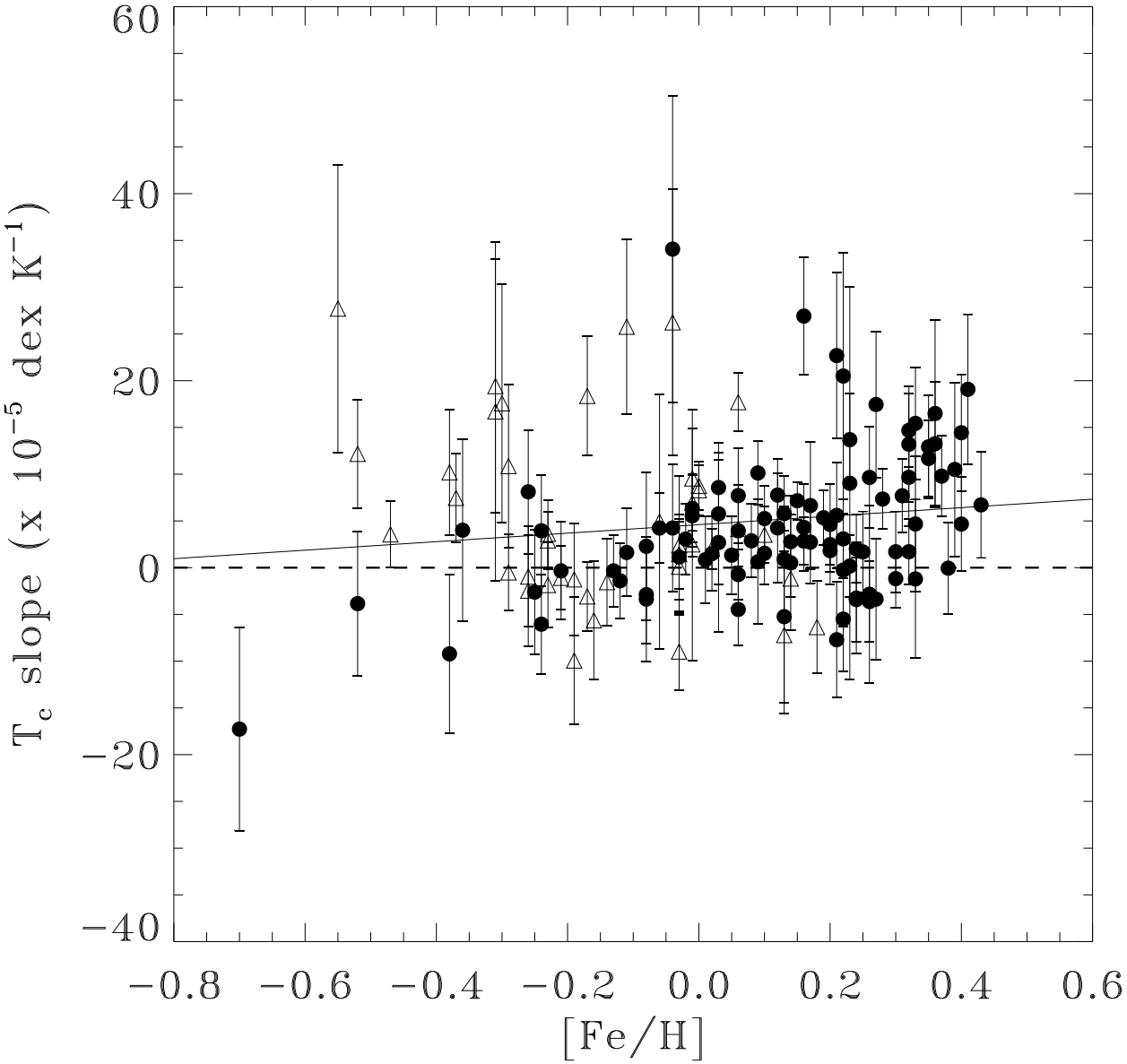
60
40
20
0
−20
−40
−0.8
−0.6
−0.4
−0.2
0.0
0.2
0.4
0.6
[Fe/H]
T_c slope (x 10^−5 dex K^−1)

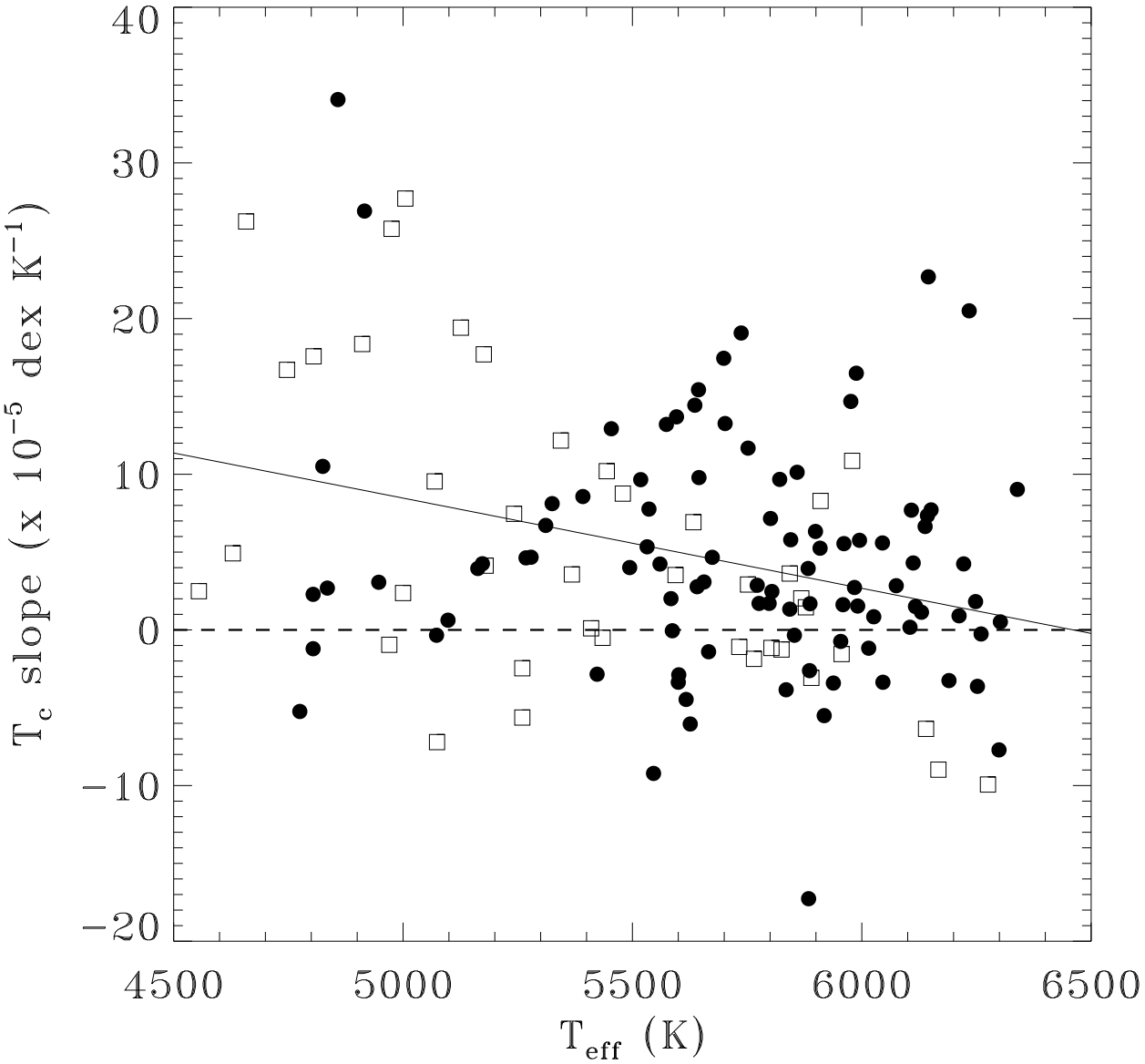
40
30
20
10
0
−10
−20
4500
5000
5500
6000
6500
T_c slope (x 10^{-5} dex K^{-1})
T_{eff} (K)

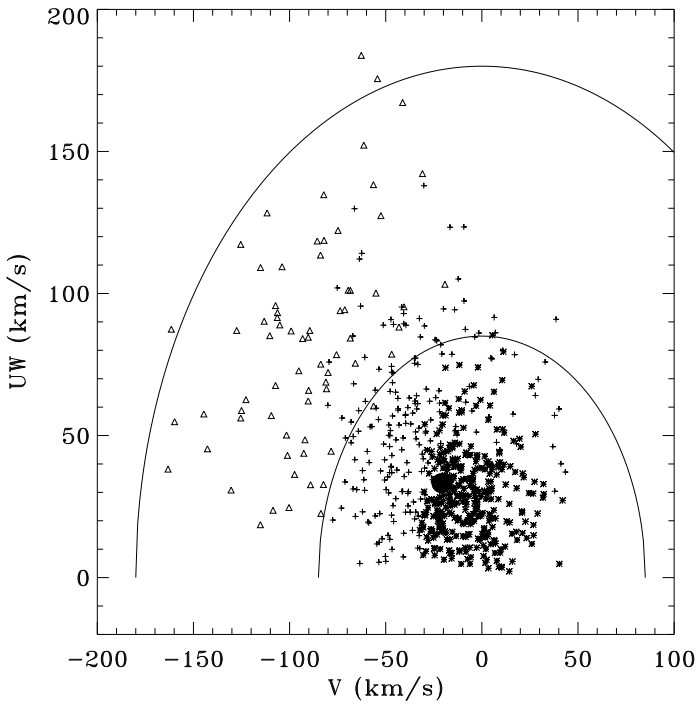
UW (km/s)
V (km/s)
200
150
100
50
0
−200
−150
−100
−50
0
50
100

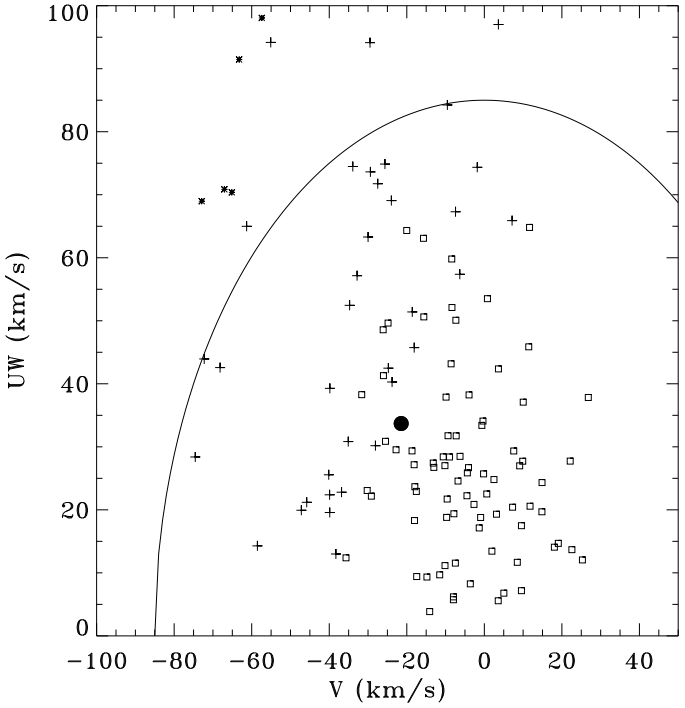
UW (km/s)
V (km/s)
100
80
60
40
20
0
−100
−80
−60
−40
−20
0
20
40

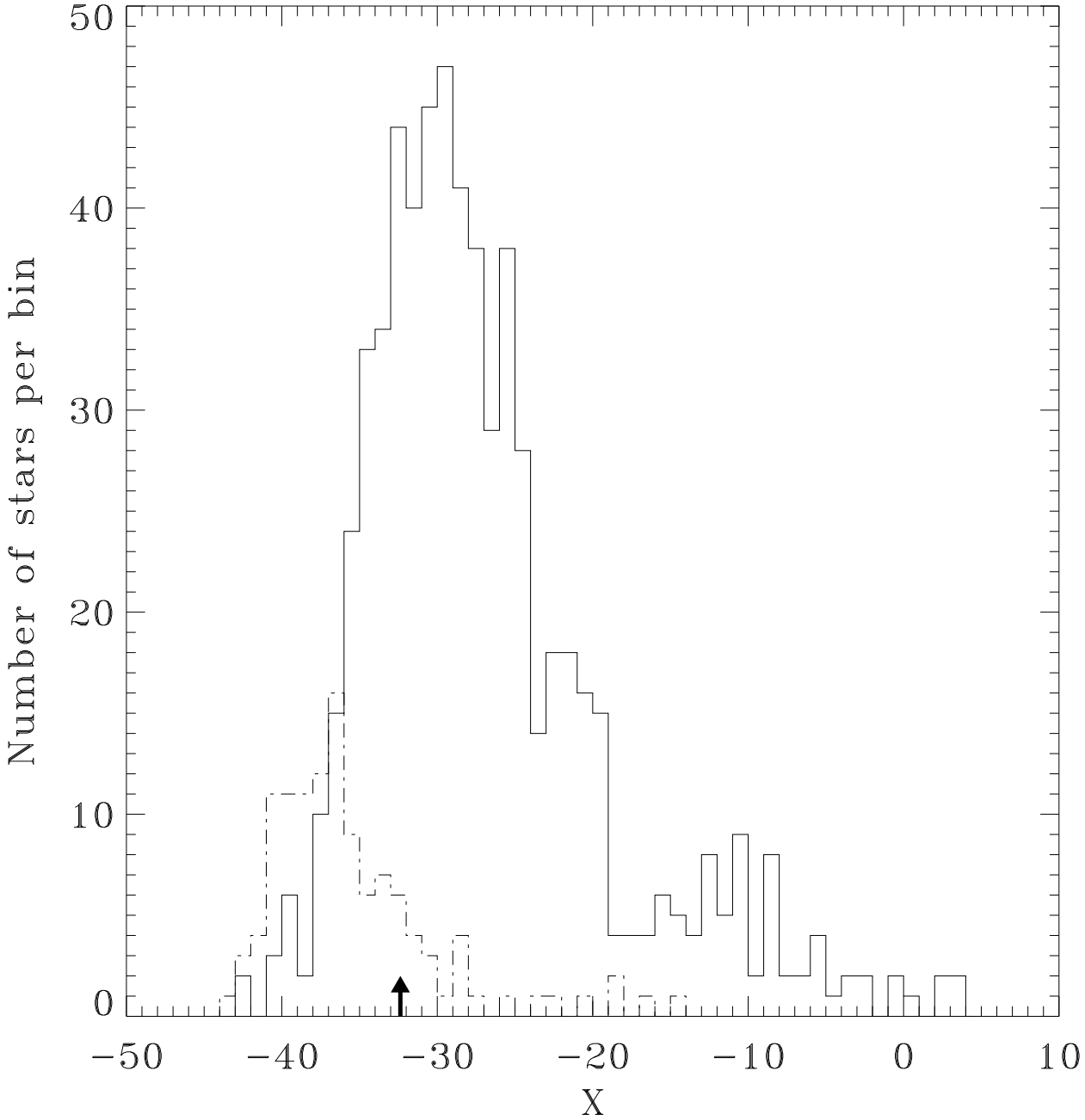
Number of stars per bin
X
50
40
30
20
10
0
−50
−40
−30
−20
−10
0
10

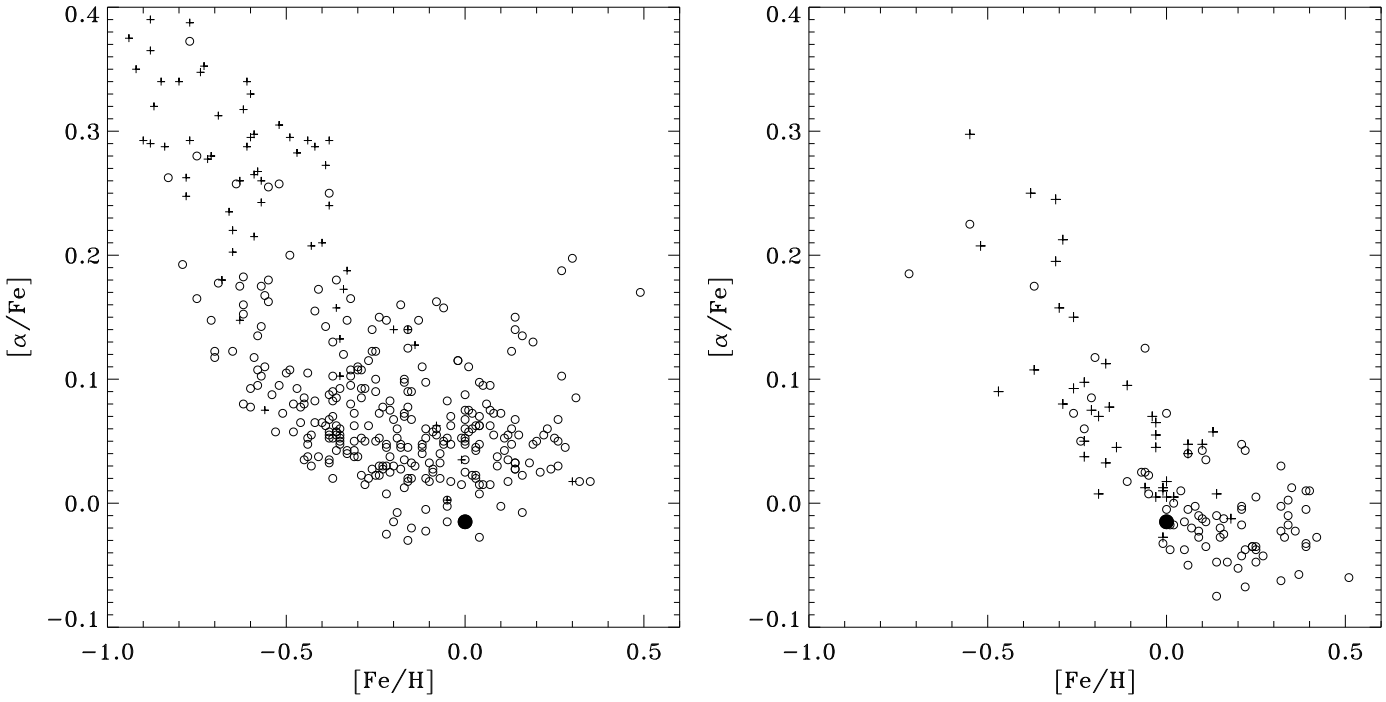
0.4
0.3
0.2
0.1
0.0
−0.1
[α/Fe]
−1.0
−0.5
0.0
0.5
[Fe/H]
0.4
0.3
0.2
0.1
0.0
−0.1
[α/Fe]
−1.0
−0.5
0.0
0.5
[Fe/H]

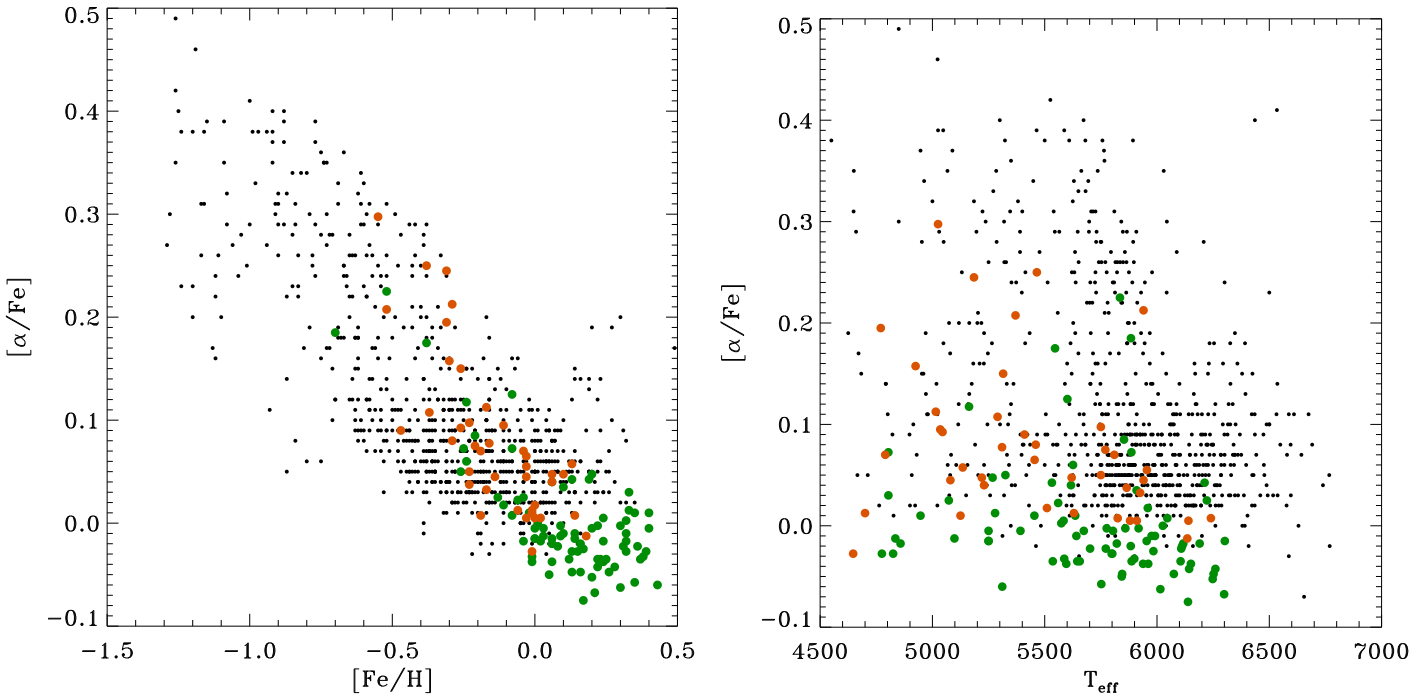
0.5
0.4
0.3
0.2
0.1
0.0
−0.1
[α/Fe]
−1.5
−1.0
−0.5
0.0
0.5
[Fe/H]
4500
5000
5500
6000
6500
7000
T_eff

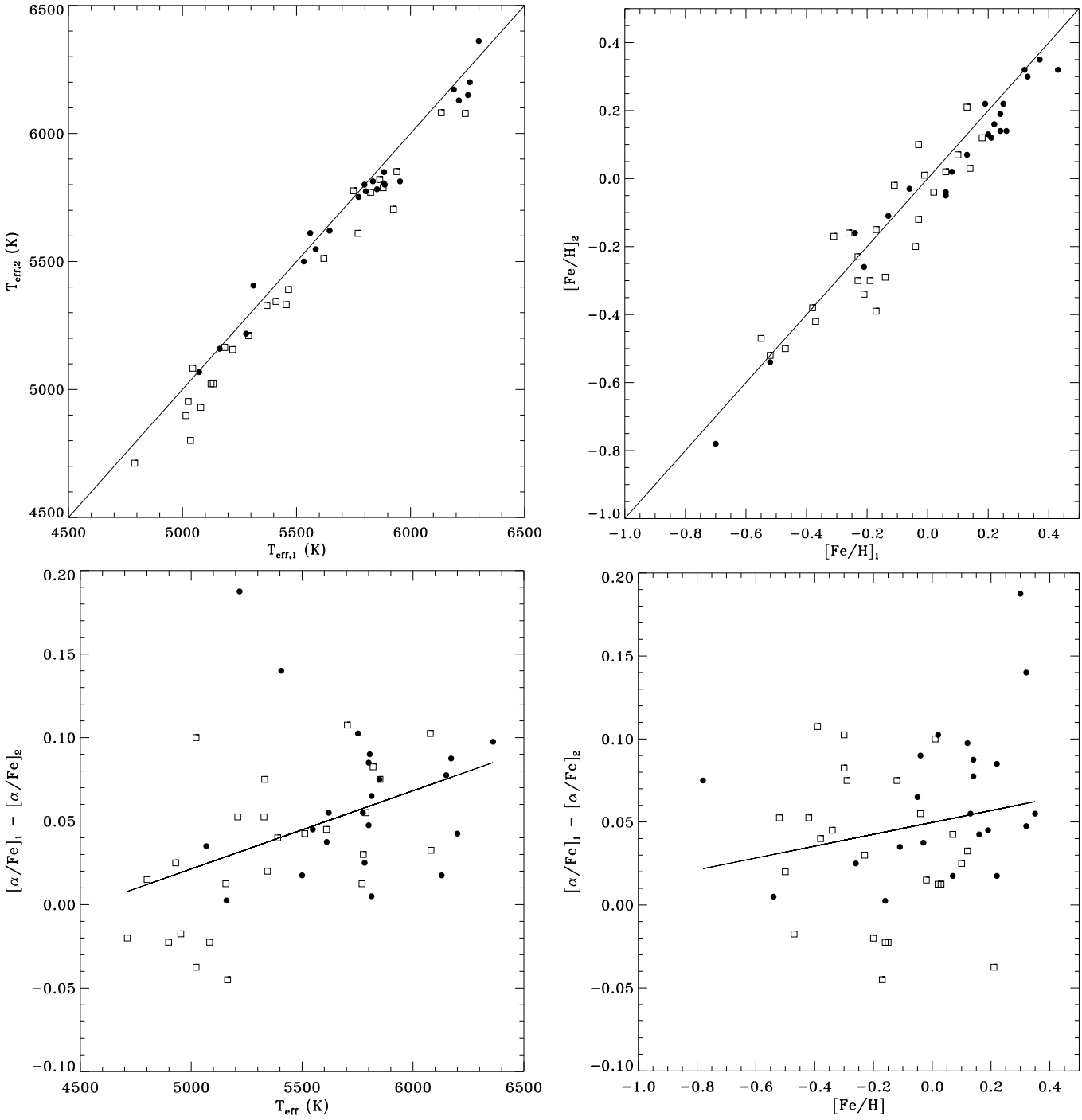
$T_{eff,2}$ (K)
$T_{eff,1}$ (K)
$[Fe/H]_2$
$[Fe/H]_1$
$[\alpha/Fe]_1 - [\alpha/Fe]_2$
T_{eff} (K)
$[\alpha/Fe]_1 - [\alpha/Fe]_2$
[Fe/H]

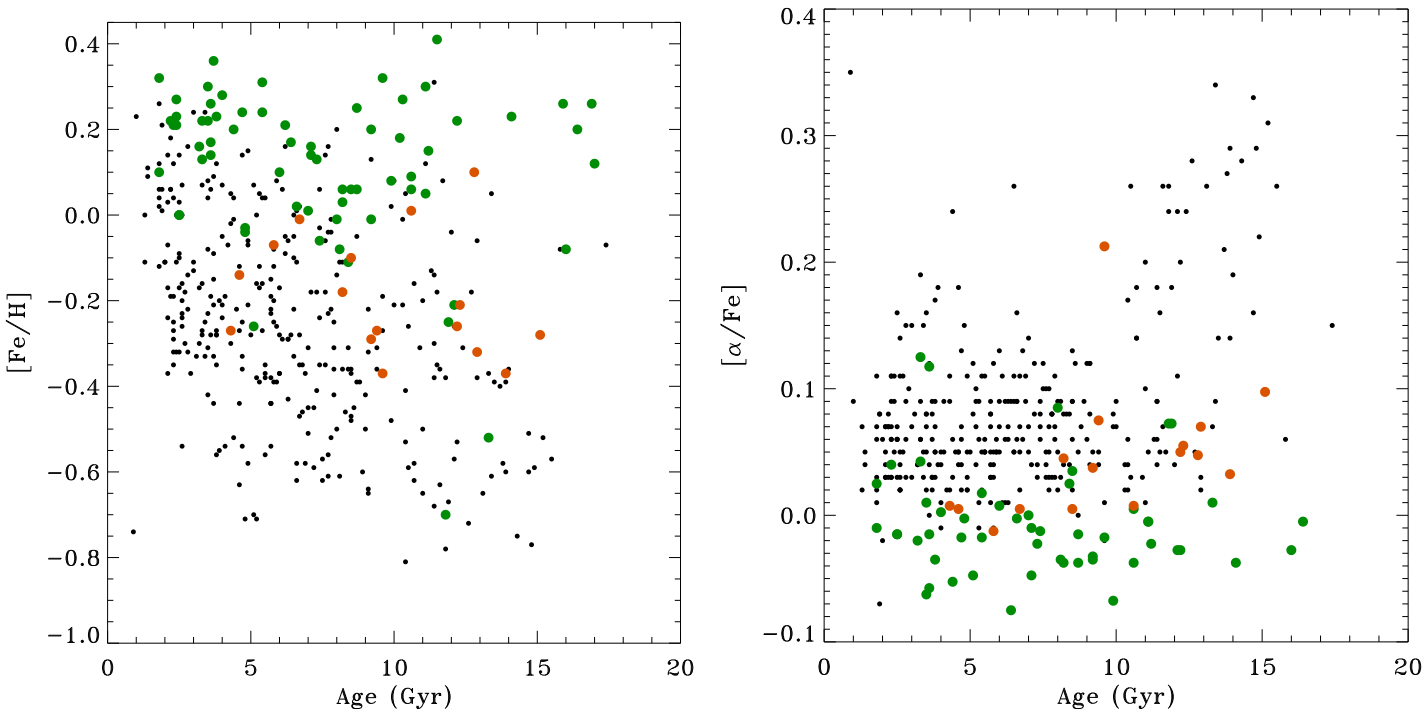
[Fe/H]
Age (Gyr)
[α/Fe]
Age (Gyr)